1 **The use of spore-pollen assemblages to reconstruct vegetation changes in the Permian**
2 **(Lopingian) Zechstein deposits of northeast England**

3 Martha E. Gibson[a*] and Charles H. Wellman[a]

4 [a]Department of Animal & Plant Sciences, University of Sheffield, Alfred Denny Building,
5 Western Bank, Sheffield S10 2TN, UK.

6 *marthae.gibson@gmail.com

7

8 ABSTRACT

9 New boreholes have enabled, for the first time, extensive palynological sampling through the
10 entire Lopingian Zechstein sequence of northeast England. Palynomorph assemblages have
11 been recovered from throughout the sequence from all five of the evaporation-replenishment
12 cycles (EZ1-EZ5). These assemblages are dominated by pollen grains, with rare trilete spores,
13 and even rarer marine forms such as acritarchs and foraminiferal test linings. The assemblage
14 of pollen grains is of low diversity (35 species) and dominated by taeniate and non-taeniate
15 bisaccate pollen. The assemblage varies to only a limited extent both within and between
16 cycles, although some minor variations and trends are documented. Based on the composition
17 of the dispersed spore-pollen assemblages, and previous work on the Zechstein megaflora, the
18 hinterland vegetation is interpreted as being dominated by conifers that inhabited a semi-arid
19 to arid landscape. This flora is shown to have persisted throughout the entire Zechstein
20 sequence, despite previous assertions that it disappeared as conditions became increasingly
21 drier over the course of the latest Permian.

22

23 *Key words:* palaeobotany, palynology, pollen, spores, vegetation change, Permian.

24

25 **1. Introduction**

26       The Lopingian Zechstein Sea was a large intercontinental sea located in Pangaea just
27 north of the equatorial Central Pangaean Mountain Range. A remarkable stratigraphical
28 sequence deposited in the sea is dominated by carbonate/evaporite cycles. The sequence can
29 be divided into seven cycles at the centre of the basin, although this is reduced to five cycles
30 towards the margins (EZ1-5) (Figure 1). These cycles essentially represent a sequence of large-
31 scale evaporation-replenishment events. The biota of the Zechstein Sea and surrounding
32 hinterlands is also remarkable. Marine biotas are impoverished due to high salinities. Although
33 reefs developed during the early cycles, these diminished and then vanished as conditions
34 became more saline and harsher during the later cycles. Palaeobotanical and palynological
35 studies reveal that a typical Euramerican flora occupied the hinterlands, low lying areas and
36 riparian environments around the Zechstein Sea during the early cycles (EZ1-2). However,
37 hitherto there has been little floral evidence in later cycles (EZ3-5) and it is often assumed that
38 vegetation diminished as harsher desert conditions prevailed as the climate became warmer
39 and drier. It is of particular interest that the sequence accumulated during the build up to the
40 end-Permian mass extinction (Erwin, 1993; Benton and Twitchett, 2003; Erwin, 2006; Hallam
41 and Wignall, 1997) and there is some evidence that the event may itself be reflected in the
42 highest cycle toward the centre of the basin (e.g. García-Veigas et al., 2011).

Recently, new boreholes have become available that penetrate the younger cycles (EZ3-5) at the margins of the Zechstein Sea in northeast England. These have yielded, for the first time, rich palynomorph assemblages from these younger cycles. This paper reports on a quantitative analysis of these palynomorph assemblages, in addition to those from older cycles (EZ1-2) collected at outcrop. The new data provides evidence for the nature of the hinterland vegetation from throughout all five cycles developed at the margins of the basin. This has enabled reconstruction of the vegetation changes that accompanied the evaporation-replenishment cycles observed in the sedimentary sequences.

| | Cycle | Durham Sub-basin | | Yorkshire Sub-basin | | Sequence |
|---|---|---|---|---|---|---|
| ~251 Ma | EZ5 | Bröckelschiefer | | Bröckelschiefer | | ZS7 |
| | | Roxby Formation | | Roxby Formation | | |
| | | | | Littlebeck Anhydrite Formation | | |
| | | | | Sleights Siltstone | | |
| | EZ4 | Sherburn (Anhydride) Formation | | Sneaton (Halite) Formation | | ZS6 |
| | | | | Sherburn (Anhydrite) Formation | | |
| | | | | Upgang Formation | | |
| | | Carnallitic Marl | | Carnallitic Marl | | |
| | EZ3 | Boulby Halite | | Boulby Halite | | ZS5 |
| | | Billingham Anhydrite Formation | | Billingham Anhydrite Formation | | |
| | | Seaham Formation | | Brotherton Formation | | ZS4 |
| | | | | Grauer Salzton Formation | | |
| | EZ2 | Edlington Formation | | Fordon Evaporite Formation | | |
| | | | | Edlington Formation | | |
| | | Roker Formation | Concretionary Limestone Member | Kirkham Abbey Formation | | ZS3 |
| | EZ1 | Hartlepool Anhydrite Formation | | Hayton Anhydrite | | |
| | | Ford Formation | | Cadeby Formation | Sprotbrough Member | ZS2 |
| | | Raisby Formation | | | Wetherby Member | ZS1 |
| ~258 Ma | | Marl Slate Formation | | Marl Slate Formation | | |

*(Left margin spanning column labels: Permian / Lopingian / Zechstein Group)*

Figure 1. Stratigraphy and correlation of the UK Zechstein deposits between the Durham Sub-basin and Yorkshire Sub-basin. Approximate Zechstein Group dates taken from Menning et al. (2005, 2006).

## 2. Geological Setting

In western and central Europe, a Lopingian to early Triassic marine-continental transition accumulated in the intracontinental Southern Permian Basin (SPB). The SPB evolved on the former Variscan foreland in the latest Carboniferous-early Permian (Ziegler, 1990). The depositional area has a width of ca. 600 km and trends ca. 2,500 km WNW-ESE from northeast England, stretching across the southern North Sea, and into northern Germany and Poland. The SPB is delineated by several Variscan Highs including the London–Brabant, Rhenish and Bohemian massifs in the south, and the Mid North Sea, and Ringkøbing–Fyn highs in the north (Ziegler, 1990; Geluk, 2005; Peryt et al., 2010).

Within the SPB tectonism initially had a relatively minor influence on the deposition of the Lopingian-early Triassic deposits. Rather, evolution of the SPB is considered to have been influenced by thermal relaxation of the lithosphere (van Wees et al., 2000) causing differential subsidence across the basin. However, the role of tectonism increased in importance in the latest Permian-earliest Triassic (uppermost Zechstein-Buntsandstein) when tectonic pulses began to affect sedimentary successions.

The initial transgression of the Zechstein Sea was a consequence of rifting in the Arctic-North Atlantic, accompanied by a contemporaneous rise in global sea levels. This resulted in flooding of the SPB via the Viking Graben System (Ziegler, 1990). Although this flooding pathway had existed previously and was responsible for minor and short-lived marine incursions during the middle Permian Upper Rotliegend (Legler and Schneider, 2008), the initial Zechstein transgression was a much more catastrophic flooding event. It is represented by the deposition of the 'Kupferschiefer' (copper shale), or Marl Slate in the UK, which indicates permanent flooding of the sub-sea-level SPB (Glennie and Buller, 1983; van Wees et al., 2000).

The Kupferschiefer/Marl Slate was deposited under basin-wide euxinic conditions (Pancost et al., 2002; Paul, 2006) and is a 0.5 m thick layer of black shale across the basin that provides an excellent marker horizon utilised in regional correlation (Geluk, 2005; Doornenbal and Stevenson, 2010). A Re-Os age of $257.3 \pm 1.6$ Ma for the Kupferschiefer in central Germany (Brauns et al., 2003) indicates a Lopingian (early Wuchiapingian) age for the basal Zechstein. However, this Re-Os age has been challenged (Słowakiewicz et al., 2009). Dating of the Zechstein in central Germany places the Zechstein Transgression at 258 Ma (Menning et al., 2005, 2006) (Figure 1).

During the Lopingian the SPB was located within the supercontinent Pangaea in the northern hemisphere desert belt at 10-30°N (Glennie, 1983). Zechstein deposition took place under arid and semi-arid climate conditions, the influence of which is documented by up to seven cycles of sedimentation and stacked evaporation cycles (Figure 1). These provide a framework for lithostratigraphical subdivision and facilitate basin-wide correlation (Richter-Bernburg, 1955). While the Zechstein Sea existed, the SPB was filled with approximately 2000m of siliciclastics, carbonates and evaporites (Peryt et al., 2010) following the classic model of cyclical chemical precipitation in a giant saline basin of Richter-Bernburg (1955). At its maximum extent, towards the centre of the Zechstein Sea, the Zechstein Group consists of seven evaporation cycles, the Werra (Z1), Staßfurt (Z2), Leine (Z3), Aller (Z4), Ohre (Z5), Friesland (Z6) and Fulda (Z7) cycles.

The entire Zechstein sequence is considered to be of Lopingian age and accumulated within a period of 2.8-3.5 Myr (Szurlies, 2013; Menning et al., 2005), 5 Myr (Menning et al., 2006), or up to 9 Myr (Słowakiewicz et al., 2009) (Figure 1). There is no consensus yet for one timescale for all of the Zechstein sequence and it is likely that different regions of the basin were deposited at different times. The British Zechstein is yet to be dated and, so far, attempts to match the Zechstein in the UK to the global chronostratigraphic timescale have been unsuccessful (D. Grocke pers. comm.). Consequently, the dates presented here are based on the latest magnetostratigraphical dating from the German/Dutch Zechstein successions (i.e. Szurlies, 2013) and carbon isotope studies (e.g. Słowakiewicz et al., 2009).

The UK Zechstein crops out over northeast England from Country Durham south to Nottinghamshire (Figure 2). These deposits accumulated in two sub-basins, separated by the Cleveland High, which ran along the western margin of the sea: the Yorkshire Sub-basin to the south and the Durham Sub-basin to the north (Smith, 1989). The sequence is divided into five evaporation cycles represented by EZ1-5 (Figure 1). The Zechstein Group is separated from the deposits of the Bakevellia Sea to the west by the low-lying, gently undulating topography of the Protopennines (Stone et al., 2010).

The Zechstein displays an overall regressive and hypersaline trend, with the thickness of strata thinning towards the margins of the SPB. As such, only the first three cycles display a full cycle of lithologies including marine clastics, carbonates and evaporites. The upper cycles

118　are dominated by clay and siltstones and generally contain fewer evaporites. These evaporites
119　formed in more localised depressions and do not extend basin-wide (Smith, 1989).

120　　The Kupferschiefer (Marl Slate) represents one of three regionally extensive marker
121　horizons used in correlation of the Zechstein (Geluk, 2005), the others being the 'Grauer
122　Salzton' (Grey Salt Clay/Illitic Shale) at the base of Z3, and the 'Roter Salzton' (Red Salt
123　Clay/Carnallitic Marl Formation) at the base of Z4. All three markers are assumed to represent
124　nearly synchronous flooding events (Doornenbal and Stevenson, 2010).

125　　Zechstein lithostratigraphy is well-defined and correlated throughout the interior of the
126　SPB for cycles Z1 to Z3. However, correlation of the upper Zechstein is more difficult with
127　disagreement regarding correlation of the Z4 of Poland (PZ4a-e) with Z5-lower Z7 in Germany
128　(Wagner and Peryt, 1997; Käding, 2000; Peryt et al., 2010). In Germany, the Zechstein-
129　Buntsandstein boundary is placed at the base of the first prominent sandstone directly above
130　the Z7 Formation (Röhling, 1993 and references therein).

131　　Zechstein deposition terminated when the connection with the Boreal Ocean was
132　interrupted by major clastic influx into the SPB (Ziegler, 1990). The SPB initially transitioned
133　into an extensive sabkha environment with isolated salinas, later becoming an extensive inland
134　playa lake in which the Lower Buntsandstein Subgroup was deposited (Hug, 2004; Hug and
135　Gaupp, 2006). Salt precipitation progressively retreated further into the basin centre during the
136　uppermost Zechstein. Tectonism resulted in downwarping of the central parts of the basin with
137　uplift creating minor unconformities at its margins (Geluk, 1999). Zechstein sedimentation
138　finally ended with the progradation of the uppermost part of EZ5/Z7, a sequence of fine-grained
139　clastic facies formerly named the 'Bröckelschiefer' (Peryt et al., 2010).

140　　Figure 1 illustrates the general stratigraphical sequence of the Zechstein of northeast
141　England. Figure 2 illustrates the location of the Zechstein sequences analysed in this study and
142　Figure 3 illustrates the stratigraphy and correlation of the Zechstein sequences. Full
143　lithostratigraphical and facies descriptions are provided in Appendix A of the online
144　supplementary information. It is important to note that in northeast England only Cycles 1-3
145　are exposed. Later cycles (Cycles 4-5) and the Permian-Triassic boundary can only be accessed
146　by boreholes and are comparatively understudied.

147

## 3. Previous palaeobotanical and palynological studies

149　　The palaeobotany of the British Zechstein sequence is well documented and comprises
150　a typical Euramerican flora dominated by gymnosperms (Stoneley, 1958; Schweitzer, 1986;
151　Cleal and Thomas, 1995). Rich palynomorph assemblages have previously been described
152　from the Zechstein of northeastern England (Wall and Downie, 1963; Clarke, 1965) as well as
153　equivalent deposits from the Bakevillia Sea of northwest England (Clarke, 1965; Warrington,
154　2008) and the Kings Court outlier in Ireland (Visscher, 1971, 1972). The palynology of other
155　Permian strata in the UK has been reviewed by Warrington and Scrivener (1988) and
156　Warrington (2005). All of these studies report mainly pollen assemblages (with subsidiary
157　spores) but include rare evidence for marine elements such as acritarchs and foraminiferal test
158　linings.

159　　Wall and Downie (1963) reported the presence of marine acritarchs in Zechstein
160　deposits from Ashfield Brick Pit, Conisborough, Yorkshire. They were rare, with the
161　assemblages dominated by pollen, and included relatively simple forms such as *Veryhachium*
162　and *Micrystridium*.

The most comprehensive review of British Zechstein palynology is Clarke (1965). Spore-pollen assemblages from the Hilton Plant Beds, Kimberley Railway Cutting and Haughton Hall Boring in Nottinghamshire were reviewed. Thirty-three taxa were reported, with assemblages containing an overwhelming dominance of *Lueckisporites virkkiae*, with *Taeniaesporites noviaulensis* and *T. labdacus* also being very abundant. Clarke reported that the most common non-taeniate taxa were *Klausipollenites schaubergeri*, *Falcisporites zapfei*, *Labiisporites granulatus* and *Illinites delasaucei*. Monosaccate pollen were represented by *Perisaccus granulosus*, *P. laciniatus*, *Potonieisporites novicus*, *Vestigisporites minutus* and *Nuskoisporites dulhuntyi*, although none of these species are common. Monosulcates are only represented by the genus *Cycadopites*. Clarke suggested that the similarity seen between Zechstein assemblages and other co-eval assemblages from the UK indicated that the Lopingian vegetation was fairly uniform throughout this region. Due to the palynological assemblages being derived from a very limited stratigraphical range it was not possible for Clarke to comment on any temporal variation. Clarke also erected three variants of *L. virkkiae* based on gross morphological differences. According to Clarke (1965) Variant A is the largest and is described as having well-developed, distinctly separate proximal thickenings and well-developed sacci, being most similar to the holotype and *L. microgra\nulatus* Klaus 1963. Variant B has sacci that are less well-developed and a small saccus offlap, being most similar to *L. parvus* Klaus 1963. Variant C has a weakly developed proximal cap that is not completely separated into two halves and is generally smaller with a more elongate corpus, being most similar to *L. microgra\nulatus* "kleinere variante" Klaus 1963.

Visscher (1971) reviewed the Permian and Triassic palynology of the Kingscourt Outlier, Ireland, which is a correlative of the Bakevellia and Zechstein seas. The oldest assemblage described (Assemblage 1) was found to closely correlate with Lopingian Zechstein assemblages from western Europe. This assemblage is dominated by *Lueckisporites virkkiae*, *Jugasporites delasaucei*, *Klausipollenites schaubergeri* and *Limitisporites moerensis*. *Perisaccus granulatus* and *Striatisaccus* sp. are minor components. However, typical Zechstein forms *Falcisporites zapfei* (Potonié and Klaus, 1954), *Labiisporites granulatus* and *Striatopodocarpites richteri* were notably absent, presumably due to the semi-isolated nature of deposits of the Kingscourt Outlier to the west of the Zechstein Basin. Visscher proposed a zonation, based on 'palynodemes' of *L. virkkiae*, which represents a rare attempt to apply a palynology-based biostratigraphy to the Zechstein Group.

More recent work on the Permian palynology of the UK has tended to focus on equivalents of the Zechstein deposits (Warrington and Scrivener, 1988; Legler et al., 2005; Legler and Schneider, 2008; Warrington, 2005, 2008). For example, the Lopingian of Devon yields poorly preserved bisaccate gymnosperm pollen (Warrington and Scrivener, 1988). *Lueckisporites virkkiae*, *Perisaccus granulosus*, *Klausipollenites schaubergeri*, *Jugasporites delasaucei*, *Protohaploxypinus microcorpus* and *Lunatisporites* spp. are found and are all compatible with a Lopingian age. The Hilton Borehole, in the Valley of Eden in Cumbria, yields the longest continuous section of Permian rocks in Britain and includes strata equivalent to the Zechstein succession (EZ1) of eastern England (Jackson and Johnson, 1996). Warrington (2008) described palynomorph assemblages, dominated by pollen, but also containing algal remains. *Crucisaccates* cf. *variosulcatus* and possibly *Proprisporites pococki* were reported for the first time from the Upper Permian of the UK.
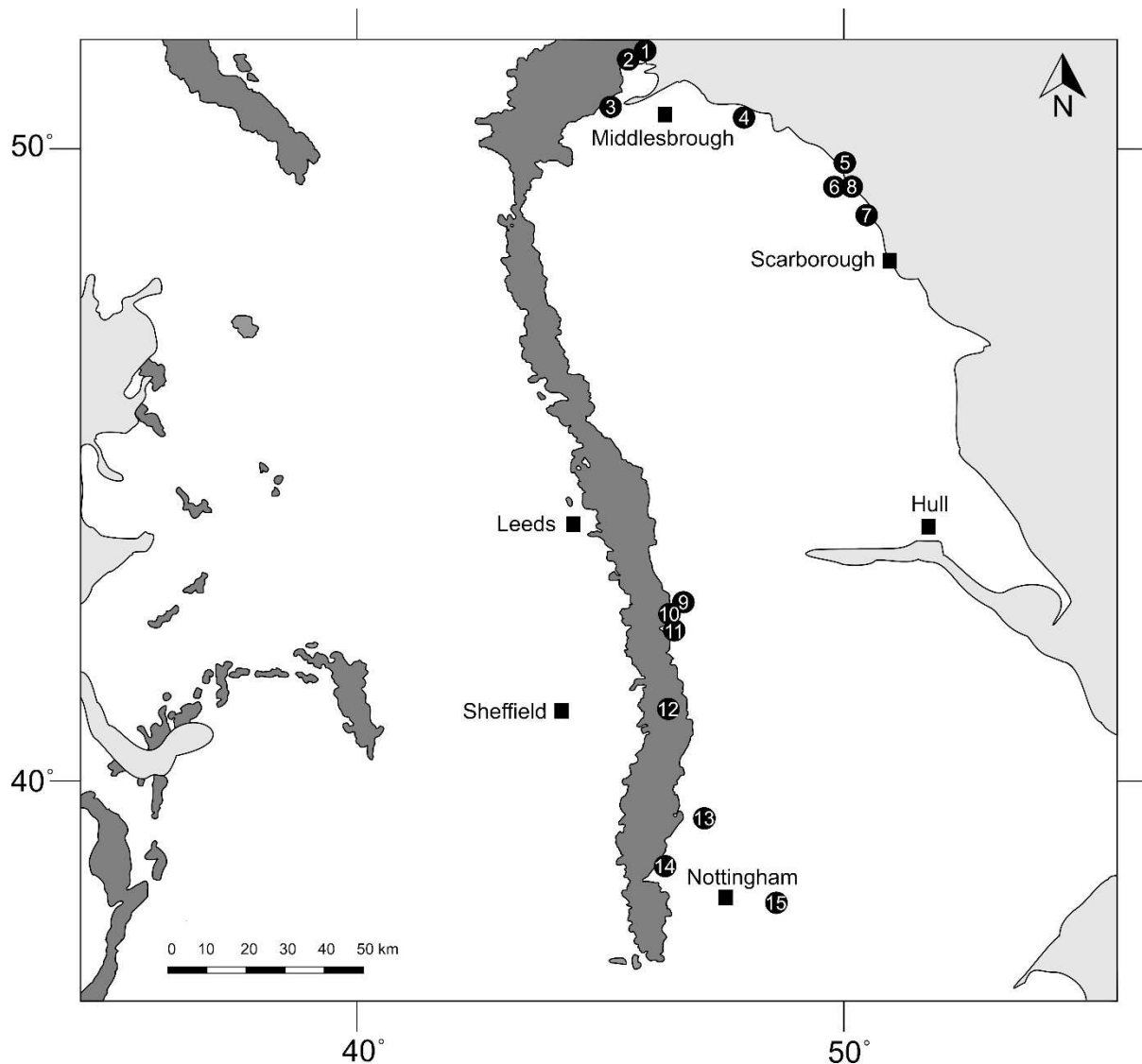
Figure 2. Outcrop map of the UK Zechstein deposits showing the location of the boreholes and outcrop exposures considered in this paper. 1) Marsden Bay, 2) Claxheugh Rock, 3) Crime Rigg Quarry, 4) Little Scar, 5) SM7 Mortar Hall, 6) SM11 Dove's Nest, 7) SM4 Gough, 8) SM14b Woodsmith Mine, 9) Pot Riding, 10) Levitt Hagg Hole, 11) Sandal House, 12) Ashfield Brick Pit, 13) Salterford Farm, 14) Woolsthorpe Bridge, 15) Kimberley. Permian outcrops are shaded in grey.

## 4. Materials and Methods

The Zechstein sequence of northeastern England was extensively collected from both outcrop and boreholes to gather a set of samples for palynological analysis from throughout the sequence. A total of 192 samples were collected from six boreholes (SM4 Gough, SM7 Mortar Hall, SM11 Dove's Nest, SM14b Woodsmith Mine North Shaft, Salterford Farm, Woolsthorpe Bridge) and outcrop samples from the Yorkshire Sub-basin (Kimberley Railway Cutting, Levitt Hagg Hole and Little Scar beach) and from the Durham Sub-basin (Claxheugh Rock, Crime Rigg Quarry and Marsden Bay). Figure 1 shows the location of the boreholes and outcrops discussed in this study. See Appendix B of the online supplementary information for

224 a list of the borehole samples and their lithology, and Appendix C for a list of the outcrop
225 samples. Appendix D provides more details of the stratigraphic range of the sampled
226 localities/boreholes. The sampling resolution was determined by the frequency of lithologies
227 suitable for palynomorph preservation and by the extent of exposed sections/borehole material
228 available for sampling.

229     The samples were palynologically processed using different techniques depending on
230 whether the lithology was clastic-carbonate or evaporite. For clastic-carbonate lithologies 20g
231 of sample was prepared using standard palynological HCl-HF-HCl acid maceration techniques.
232 The residue was first top sieved at 10µm to detect the presence of acritarchs, then at 20µm, and
233 subjected to heavy liquid separation using zinc chloride to extract and concentrate the organic
234 residues. Evaporite lithologies were processed according to the method outlined in Gibson and
235 Bodman (2020), whereby samples are dissolved in hot water, boiled in concentrated 40% HF
236 for 15 minutes to remove any remaining clastics, then subjected to heavy liquid separation
237 using zinc chloride to extract and further concentrate any organic residue.

238     For productive samples, the residues varied considerably in palynomorph
239 colour/opacity. In most samples the palynomorphs were beautifully preserved and of very low
240 thermal maturity (translucent yellow-orange). In some samples the palynomorphs were of very
241 low thermal maturity and appeared hyaline (e.g. Marl Slate of the Durham Sub-basin). These
242 were stained using Bismark Brown to improve contrast and visibility of palynomorphs. On the
243 other hand, samples associated with evaporites were often opaque dark brown-black
244 (frequently 98-100% PDI) (Goodhue and Clayton, 2010; Clayton et al., 2017). This darkening
245 is unlikely to be due to high thermal maturity as the Zechstein deposits have not been subjected
246 to deep burial and high heat flow and palynomorph assemblages above and below are of very
247 low thermal maturity (see Gibson and Bodman (2020)). It appears to result from a diagenetic
248 effect of preservation within evaporites. Where necessary, samples were oxidized using
249 Schulze's reagent for up to 26 hours which cleared the palynomorphs to translucent orange.
250 Samples containing large quantities of amorphous organic matter (AOM) were treated with
251 pulsed ultrasound treatment to break up the AOM and prevent it from obscuring palynomorphs
252 during analysis. The organic residue was strew mounted onto glass slides for light-microscopic
253 (LM) analysis.

254     Specimens were analysed and photographed using a QImaging (Model No. 01-MP3.3-
255 RTV-R-CLR-10) camera mounted on an Olympus BH-2 transmitted light microscope in
256 conjunction with QCapture Pro software. All samples, residues, and LM slides are curated in
257 the Centre for Palynology at the University of Sheffield, UK.

258     Once a taxonomy had been established (at least one slide was logged for each sample
259 recording all taxa present) a minimum count was made for each sample. If sufficient
260 palynomorphs were present a minimum count of 200 was undertaken. When there were
261 insufficient palynomorphs the entire palynomorph population was counted. To accommodate
262 for differences in quantitative approach, samples containing a yield greater than 200 were
263 rarefied to 200. Damaged grains (>50%) identifiable as bisaccate or monosaccate pollen grains
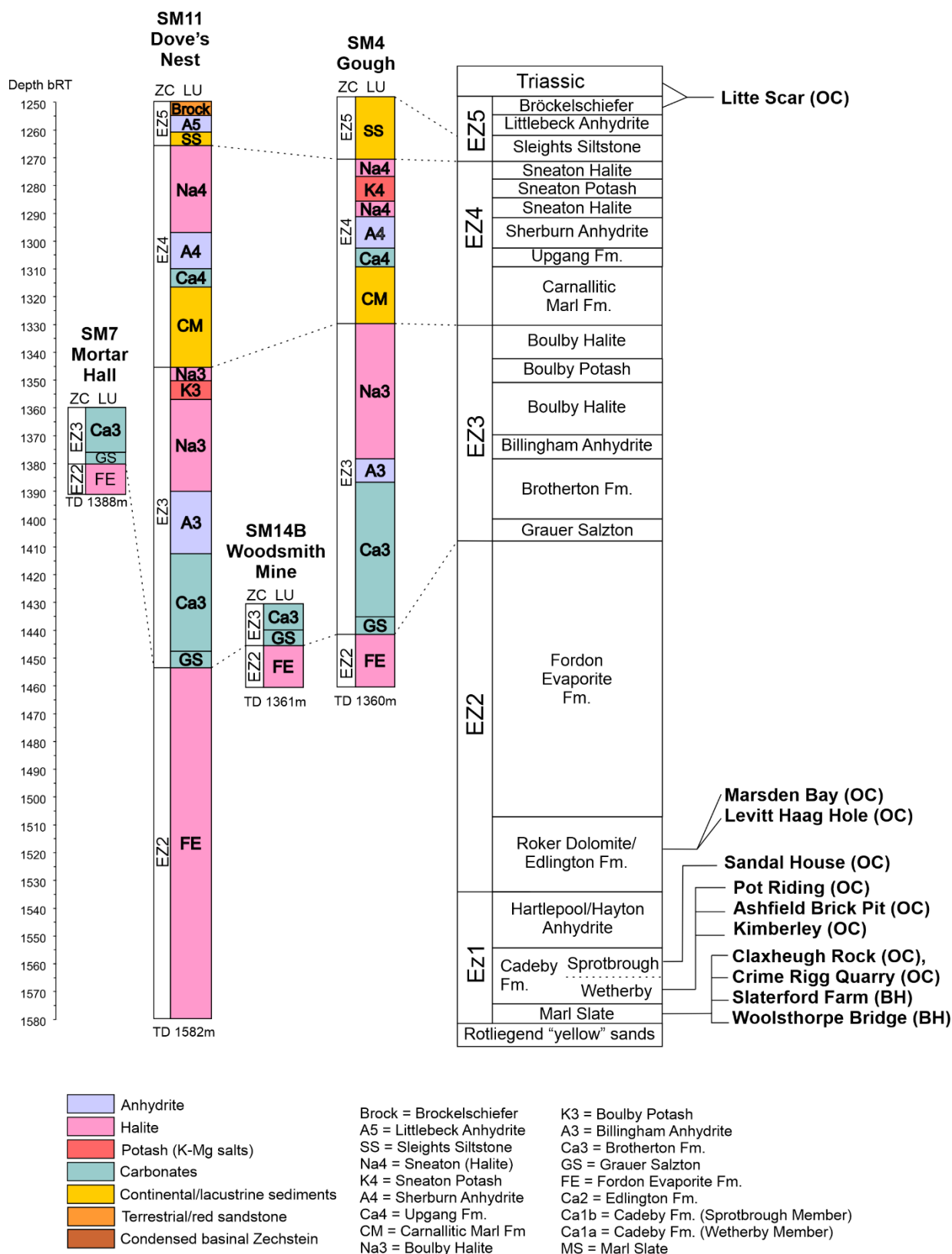
266    Figure 3. Stratigraphy and correlation of the sequences analysed in this study. OC = Outcrop,
267    BH = borehole, ZC = Zechstein cycle, LU = Lithostratigraphic unit, and TD = Terminal Depth
268    (m) of commercial boreholes. C = carbonates and E = evaporites.

## 5. Palynological results

269

270     Recovery was highly variable from the different lithologies sampled. Many of the
271 clastic deposits yield abundant organic residue containing rich and diverse assemblages of
272 well-preserved palynomorphs of low thermal maturity. Most of the evaporite deposits produced
273 very low yields of organic residue, although these often contained palynomorphs. However,
274 palynomorphs from the evaporites were variable in preservation, varying both in quality of
275 preservation (excellent to poor) and colour (translucent pale yellow to opaque black). All of
276 the palynological samples were dominated by pollen, with very rare spores, and only occasional
277 marine forms (acritarchs and foraminiferal test linings). A list of the taxa encountered is
278 provided in Table 1 and illustrations of these taxa are in Plates I-III. Figures 4-14 illustrate the
279 palynomorph occurrence and distribution for each locality. The raw data is provided in
280 Appendix E. Table 2 summarises the palynomorph distribution.

281
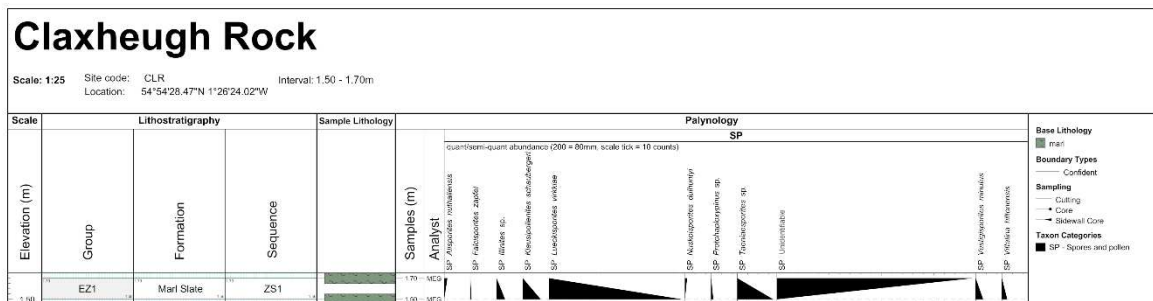
282



283     Figure 4. Occurrence and distribution of palynomorphs from Claxheugh Rock.
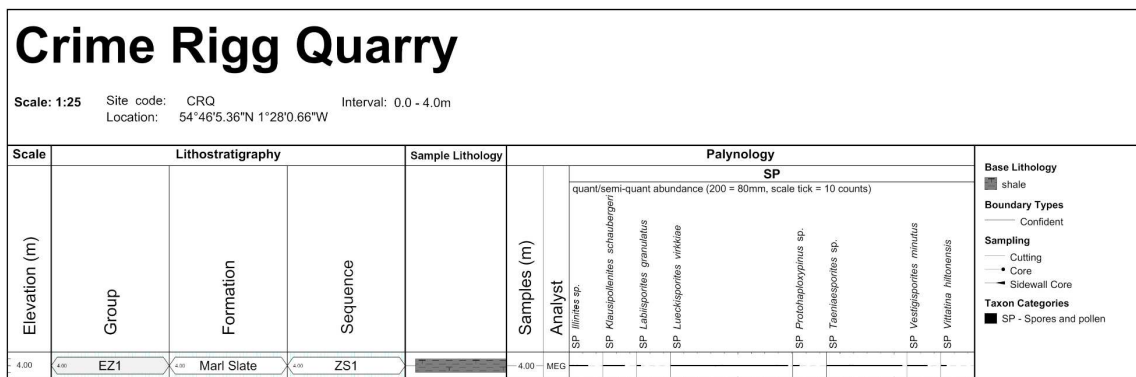


284

285     Figure 5. Occurrence and distribution of palynomorphs from Crime Rigg Quarry.

286

287    Figure 6. Occurrence and distribution of palynomorphs from Kimberley.



288

289    Figure 7. Occurrence and distribution of palynomorphs from Salterford Farm.



290

291    Figure 8. Occurrence and distribution of palynomorphs from Woolsthorpe Bridge.

292

293

Figure 9. Occurrence and distribution of palynomorphs from Marsden Bay.



295

Figure 10. Occurrence and distribution of palynomorphs from SM4 Gough.

297

# SM11 Dove`s Nest

Scale: 1:275  Well Code: SM11DOVESNEST  Location: 54°26'7.652"N 0°37'22.006"W
Operator: York Potash Ltd  Interval: 1249m - 1582m

298

**SM11 Dove's Nest**

299

300

301　Figure 11. Occurrence and distribution of palynomorphs from SM11 Dove's Nest.
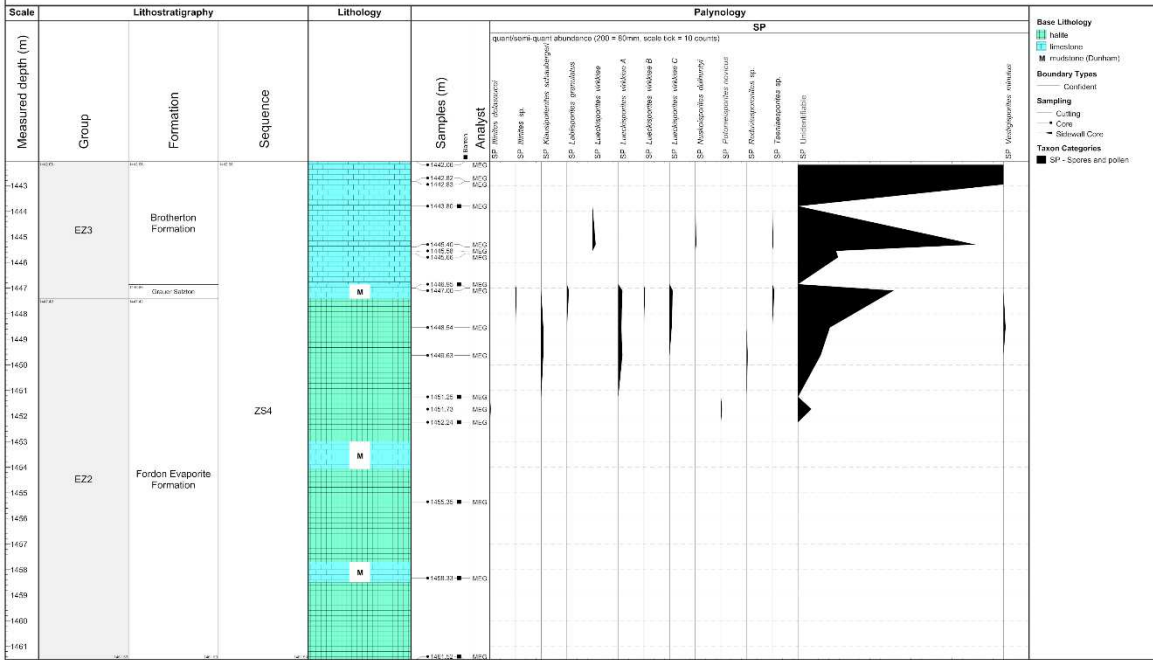
302

303     Figure 12. Occurrence and distribution of palynomorphs from SM14b Woodsmith Mine.
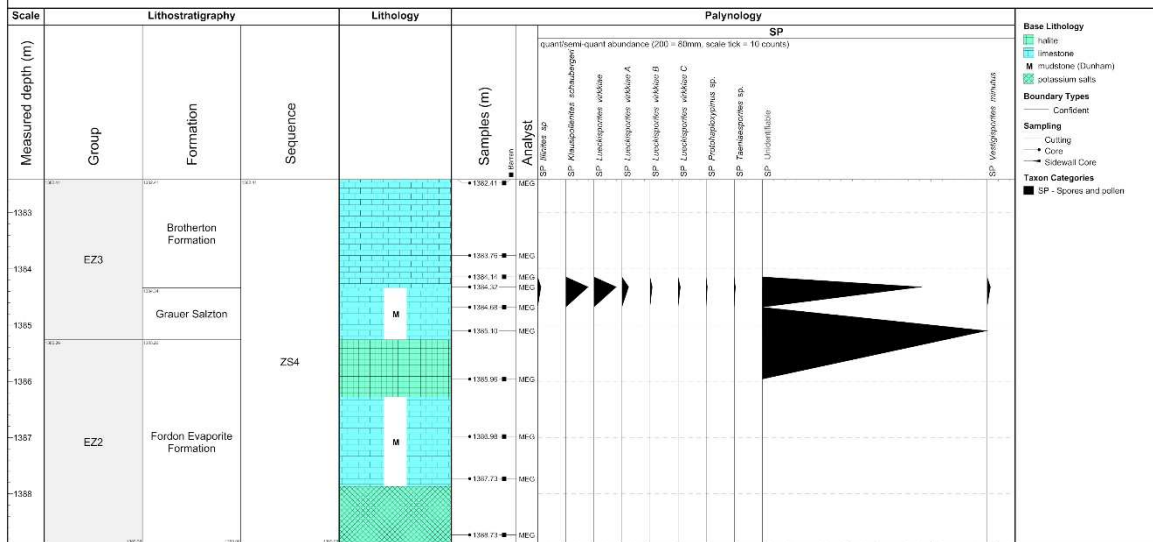


304

305     Figure 13. Occurrence and distribution of palynomorphs from SM7 Mortar Hall.

306

**Little Scar**

Scale: 1:150    Site code:    LSSC    Interval: 2.0 - 18.0m
Location:    54°39'46.6"N 1°11'12.0"W

| Scale | Lithostratigraphy | Sample Lithology | Palynology | | Text Keys |
|---|---|---|---|---|---|

Palynology columns: SP, FOP

Text Keys
*1 quant/semi-quant abundan...

**Base Lithology**
M mudstone (Dunham)
siltstone

**Boundary Types**
—— Confident

**Sampling**
Cutting
Core
Sidewall Core

**Taxon Categories**
■ SP - Spores and pollen

Elevation (m) — Group

Samples (m) — Analyst — SP *Taeniaesporites* sp. — SP *Trisaccate* sp. — FOP Foraminiferal test linings

Bröckelschiefer (P-T boundary)

Zechstein

16.90 ■ MEG
16.60 ■ MEG
16.30 — MEG

8.00 ■ MEG

5.50 — MEG
5.00 — MEG
4.50 — MEG
4.00 — MEG
3.50 — MEG
3.00 — MEG
2.00 ■ MEG

Figure 14. Occurrence and distribution of palynomorphs from Little Scar.

## 5.1. General description of the spore/pollen assemblages

The assemblages are often dominated by the taeniate bisaccate *Lueckisporites virkkiae* (Plate I, 1-5) occurring at sufficient frequencies to dominate assemblages by ~50.0%. Variant A (Plate I, 1, 2) is the most common variant, averaging 9.9-26.8% of assemblages, with Variant B (Plate I, 3) and Variant C (Plate I, 4, 5) being noticeably less abundance, 1.7-5.1% and 1.5-9.4% respectively. *L. virkkiae* maintains dominance throughout the Zechstein sequence.

*Taeniaesporites* spp. (Plate I, 6-12), the most common species of which is *T. labdacus* (up to 14.0%, average 0.7-5.9%) (Plate I, 6, 7), is present up until the Cycle 4 carbonates but no later. Average abundance ranges between 1.3-22.5%, with maximum abundance achieved in the Marl Slate. *Protohaploxypinus* spp. (Plate I, 13-16), the most common of which are *P. chaloneri* (Plate I, 13, 14) and *P. jacobii* (Plate I, 15, 16), has a slightly greater temporal range than *Taeniaesporites*, and is present into the Cycle 4 evaporites. *Protohaploxypinus* spp. ranges in abundance from 0.6-2.2% of assemblages, but individual species can reach abundances of 3.4% (e.g. *P. jacobii* in the Cycle 3 evaporites). The presence and abundance of other taeniate species is also as expected from Lopingian assemblages. The distinct asaccate species *Vittatina*

325 *hiltonensis* (Plate II, 1, 2) maintains a rare abundance throughout of 0.5-3.17%. *Striatioabietites*
326 (Plate II, 3) and *Striatopodocarpites* (Plate II, 4, 5) occur at low abundances only, typically
327 <0.5% of the assemblages, but up to 2.0% in the Cycle 3 evaporites. *Platysaccus radialis* (Plate
328 II, 6) is a rare bisaccate only occurring in the Cycle 1 carbonates (1.0%) and very rare in the
329 Cycle 4 carbonates (<0.5%).

330      Regarding non-taeniate bisaccate pollen, *Klausipollenites schaubergeri* (Plate II, 7, 8)
331 is the most abundant and is present from the Marl Slate through to the Cycle 4 evaporites. It is
332 similar in morphology to *Vestigisporites minutus* (Plate II, 9-11), but distinctly bisaccate rather
333 than monosaccate and larger in size. *K. schaubergeri* exhibits a large range in abundance but
334 on average represents between 5.8-20.0% of assemblages. A maximum abundance of 27.0% is
335 achieved in the Cycle 2 carbonates, but abundances can be as low as 0.5%. *Illinites* spp. (Plate
336 II, 12-15) is the only other pollen grain taxon to occur in the Cycle 5 evaporites alongside
337 *Lueckisporites virkkiae*, however it is absent in the Cycle 4 evaporites and Cycle 5 carbonates.
338 It is easily identifiable with its distinct corpus and sacci shape meaning its presence can be
339 recorded even in poorly preserved samples. *Illinites* spp. is represented by three species, with
340 *I. delasaucei* (Plate II, 12) being the most common (0.5-6.5%) and *I. klausi* (<0.5-3.5%) (Plate
341 II, 13) and *I. tectus* (0.5-5.2%) (Plate II, 14, 15) being present at lower abundances.
342 *Falcisporites zapfei* (Plate I, 12, 13) is the largest non-taeniate bisaccate recovered, occurring
343 at low abundances from the Marl Slate through to the Cycle 4 carbonates at <0.5-1.3%. The
344 distinctive bisaccate *Alisporites nuthallensis* (Plate II, 18) is present from the Marl Slate
345 through to the Cycle 4 carbonates at low abundances of 0.5-2.4%. The triangular-outlined
346 pollen species *Labiisporites granulatus* (Plate II, 19, 20) was observed at average abundances
347 of 0.5-5.1%, but with abundances as high as 18.0% in the Cycle 3 evaporites. This species
348 exhibits one of the largest variations in abundance in the studied material.

349      Large monosaccate pollen species are, as expected, rare e.g., *Nuskoisporites dulhuntyi*
350 (Plate III, 1), *N.* cf. *rotatus* (Plate III, 2), *Perisaccus granulosus* (Plate III, 3, 4) and
351 *Potonieisporites novicus* (Plate III, 5, 6). *Nuskoisporites* spp. and *P. granulosus* are present in
352 the Marl Slate through to the Cycle 4 carbonates, while *Potonieisporites novicus* has a similar
353 range yet is not present in the Marl Slate. These large monosaccate pollen typically only
354 represent 1.0-2.0% of assemblages or less. However, the small monosaccate *Vestigisporites*
355 *minutus* is one of the most common pollen species comprising on average 5.0% of assemblages.
356 *V. minutus* can comprise up to 17.5% of assemblages in Cycle 3 evaporites.

357      The possible cycad pollen, *Cycadopites rarus,* is very rare (0.5%). *C. rarus* is only
358 recorded in the Cycle 3 evaporites. Trilete spores (Plate II, 8, 9) maintain a low abundance
359 throughout Cycle 1-4 but reach their maximum presence of 13.6% in the assemblages of the
360 Cycle 4 evaporites. However, assemblages from Cycle 4 and Cycle 5 were of a lower yield
361 relative to earlier cycles. Trisaccate pollen grains are rare and may represent aberrant forms of
362 other pollen species (Foster and Afonin, 2005; Metcalfe et al., 2009). They occur at <0.5%
363 from Cycle 1 carbonates to Cycle 3 evaporites but are not found in assemblages beyond.
364 Tetrads are only found in Cycle 1 carbonates at maximum abundances of 0.5%. Cuticle
365 fragments of varying size (20-200μm) were common in assemblages, with larger fragments
366 recovered from the evaporite preparations than standard preparations.

367

368 *5.2. Description of palynomorph distribution by locality*

369

*5.2.1. Cycle 1 transgressional sediments and carbonates (EZ1 Ca) (Marl Slate and carbonates): Claxheugh Rock and Crime Rigg Quarry exposures*

Palynomorph assemblages from Cycle 1 of the Durham Sub-basin were recovered from exposures of the Marl Slate at Claxheugh Rock (Figure 4) and Crime Rigg Quarry (Figure 5). Palynological preparations contain vast amounts of amorphous organic matter (AOM). Palynomorphs are present and are well-preserved and hyaline in appearance. The hyaline nature hampered identification of palynomorphs, but genus-level identifications, and some species-level identifications of distinct taxa, were possible after samples were stained with Bismarck Brown.

The assemblages recovered from the exposure at Claxheugh Rock (Figure 4) were composed of taeniate bisaccate species: *Lueckisporites virkkiae* (31.5%), *Protohaploxypinus* sp. (1.0%), *Taeniaesporites* sp. (17.0%) and *Vittatina hiltonensis* (1.0%). Non-taeniate bisaccate species include *Alisporites nuthallensis* (<0.5%), *Illinites* sp. (2.0%), *Klausipollenites schaubergeri* (8.5%), rare *Labiisporites granulatus* (<1.0%) and *Falcisporites zapfei* (<0.5%). Rare multisaccate *Crustaesporites globosus* (<0.5%) (Plate III, 7) was present. Monosaccate pollen was represented by *Vestigisporites minutus* (3.5%) and rare *Perisaccus granulosus* (<0.5%) and *Nuskoisporites dulhuntyi* (0.5%). One sample (CLR) did not contain Unidentifiable palynomorphs but contains rare unidentifiable spores (<0.5%), while the other sample (CLR2) contains 93.0% Unidentifiable palynomorphs.

The assemblage from Crime Rigg Quarry (Figure 5) was composed of the taeniate bisaccate species *Lueckisporites virkkiae* (43.5%), *Protohaploxypinus* sp. (2.5%), rare *Striatopodocarpites* sp. (<0.5%%), *Taeniaesporites* sp. (28%), and *Vittatina hiltonensis* (2.0%), and the non-taniate bisaccate species *Illinites* sp. (7.0%), *Klausipollenites schaubergeri* (8.0%), *Labiisporites granulatus* (1.5%), *Falcisporites zapfei* (<0.5%), as well as the monosaccate pollen *Perisaccus granulosus* (<0.5%) and *Vestigisporites minutus* (7.5%).


*5.2.2. Cycle 1 transgressional sediments and carbonates (EZ1 Ca) (Cadeby Fm.: Wetherby/Sprotbrough Mb.): Kimberley railway cutting exposure and the Salterford Farm and Woolsthorpe Bridge boreholes*

Palynomorph assemblages from Cycle 1 of the Yorkshire Sub-basin were recovered from the Cadeby Fm. exposure in Kimberley railway cutting (Figure 6), Salterford Farm borehole (Figure 7), and Woolsthorpe Bridge borehole (Figure 8). The palynomorphs were well preserved and translucent. Both assemblages from Kimberley railway cutting, K5 and K6, contain *Lueckisporites virkkiae* (K5 39.0%, K6 50.0%), *Taeniaesporites* sp. (K5 2.5%, K6 1.0%), *T. labdacus* (K5 10.5%, K6 6.5%), *T. novimundi* (K5 2.5%, K6 2%), *T. noviaulensis* (K5 2.5%, K6 5.5%), *T. angulistriatus* (K5 2.0%, K6 2.0%), *T. albertae* (K6 7.5%), *Protohaploxypinus jacobii* (K5 2.0%), *Striatopodocarpites antiquus* (K5 1.0%, K6 0.5%), *Vittatina hiltonensis* (K5 2.5%), *Illinites* sp. (K5 5.5%), *I. delasaucei* (K5 9.5%, K6 8.5%), *I. klausi* (K6 3.5%), *I. tectus* (K5 1.0%, K6 0.5%), rare *Nuskoisporites dulhuntyi* (K5 <0.5%) and *Potonieisporites novicus* (K5 <0.5%), rare *Perisaccus granulosus* (K6 <0.5%), unidentifiable spores (K5 2%, K6 0.5%), and rare tetrads (K6 0.5%).

Assemblages from the Salterford Farm borehole samples were composed of the taeniate bisaccate species *Lueckisporites virkkiae* with Variant A (21.3%), Variant B (1.7%) and Variant C (2.5%), *Protohaploxypinus* sp. (0.5%) *P. chaloneri* (<0.5%), *P. jacobii* (0.5%), *Striatoabieites richteri* (0.5%), *Striatopodocarpites* sp. (0.5%), *Taeniaesporites* sp. (0.5%), *T. albertae* (0.8%), T. *angulistriatus* (0.8%), *T. bilobus* (<0.5%), *T. labdacus* (2.8%), *T.*

*novimundi* (1.3%), *T. noviaulensis* (0.8%). The non-taeniate bisaccate pollen *Alisporites nuthallensis* (2.5%), *Falcisporites zapfei* (0.9%), *Illinites delasaucei* (5.1%), *I. tectus* (0.5%), *Klausipollenites schaubergeri* (14.3%), *Labiisporites granulatus* (3.5%), *Platysaccus radialis* (1.0%) and *Potonieisporites novicus* (0.5%) were recovered. The multisaccate *Crustaesporites globosus* was recorded (0.5%). Monosaccate pollen were represented by *Nuskoisporites dulhuntyi* (0.5%), *Perisaccus granulosus* (0.6%) and *Vestigisporites minutus* (6.7%). *Reduviasporonites* sp. was found throughout (2.7%), trisaccates were rare (0.4%) and spores were found in all samples (1.6%). A solitary tetrad in YFP6368 was recovered and a single foraminiferal test lining was recovered from SF465. The Unidentifiable palynomorph component averages at 33.0%.

The sample of Marl Slate obtained from Woolsthorpe Bridge borehole (Figure 8) was not species rich and was dominated by Unidentifiable palynomorphs (56.1%). Identifiable taeniate bisaccate pollen include *Lueckisporites virkkiae* Variant A (15.8%), Variant B (1.8%) and Variant C (3.5%), *Taeniaesporites labdacus* (1.8%), *T. albertae* (3.5%), and non-taeniate bisaccate pollen include *Klausipollenites schaubergeri* (12.3%) and *Labiisporites granulatus* (1.8%). The only monosaccate taxon present was *Vestigisporites minutus* (3.5%).

The remaining Cycle 1 carbonates, sampled at Ashfield Brick Pit, Sandal House, and Pot Riding, were essentially barren of palynomorphs, containing only a few palynomorphs of such poor preservation they lacked characters that enabled them to be identified even as Unidentifiable pollen grains. Therefore, these sites were designated as barren.

*5.2.3. Cycle 1 evaporites (EZ1 A) (Hartlepool Anhydrite/Hayton Anhydrite)*

Cycle 1 evaporites were not covered in the sampling range of this study as they are not represented by any of the borehole material and they are not exposed at outcrop as a result of dissolution.

*5.2.4. Cycle 2 carbonates (EZ2 Ca) (Roker Dolomite/Edlington Fm. and Kirkham Abbey Fm.): Marsden Bay*

A sample of red mudstone from the Edlington Fm. collected from outcrop at Levitt Hagg Hole was barren of palynomorphs. Samples of Roker Dolomite Fm. from Marsden Bay (MB1-6) (Figure 9) contained taeniate and non-taeniate bisaccate pollen, as well as rare monosaccate pollen. The assemblage of MB2 was the best preserved. The taeniate bisaccate taxa were represented by *Lueckisporites virkkiae* (53.5%), and *Taeniaesporites* sp. (1.8%) is also abundant, with *T. angulistriatus* (<0.5%), *T. labdacus* (0.5%) and *T. novimundi* (<0.5%). *Protohaploxypinus* sp. (3.1%) was present, with *P. chaloneri* (<0.5%) and *P. jacobii* (<0.5%) present. *Striatopodocarpites* sp. (<0.5%) was rare and only found in one sample (MB2). *Vittatina hiltonensis* (0.9%) was present at rare abundance in MB1-3. Smooth bisaccate pollen was represented by abundant *Illinites* sp. (6.1%) with rare *I. delasaucei* (<0.5%) only recovered from MB2. *Klausipollenites schaubergeri* was abundant (23.3%), while *Labiisporites granulatus* (1.0%), *Alisporites nuthallensis* (0.9%) was uncommon, and *Falcisporites zapfei* (<0.5%) (MB4-6) and *Potonieisporites novicus* were rare (<0.5%). The monosaccate pollen *Nuskoisporites dulhuntyi*, and *Perisaccus granulosus* were rare (<0.5%), and *Vestigisporites minutus* (MB1-2) was found in MB1-2. The Unidentifiable component was only present in MB1 and only comprises 16% of the assemblage. Unidentifiable trisaccate pollen grains were recovered from MB1 (<0.5%).

461       The remaining samples from Marsden Bay (MB4-6) contained similar assemblages, but
462 typically of lower yield. MB4 contains an exceptionally well-preserved assemblage but was of
463 low yield (n=102), with *Lueckisporites virkkiae* composing 20.0% of the assemblage. There
464 were no Unidentifiable palynomorphs, but *L. virkkiae* Variant A was abundant (14.0%) while
465 Variant B was rare (<0.5%). Other taeniate genera *Taeniaesporites* sp. were present (1.8%) as
466 well as *Protohaploxypinus* spp. which was only found in MB4 (0.5%), with rare *P. chaloneri*
467 (<0.5%) and *P. microcorpus* (<0.5%) recovered from MB5. The non-taeniate bisaccate pollen
468 *Illinites* sp. (10.7%), *Falcisporites zapfei* (0.5%), and *Klausipollenites schaubergeri* (16.7%)
469 were abundant in MB4-6. The only monosaccate taxon recovered from MB4-6 was the small
470 species *Vestigisporites minutus* that was only recovered from MB5 (2.5%). Unidentifiable
471 pollen grains comprised on average 54.5% of the assemblages.

472

473 *5.2.5. Cycle 2 evaporites (EZ2 A, EZ2 K, EZ2 Na) (Fordon Evaporites Fm): SM4, SM11 and*
474 *SM14b boreholes*

475       The borehole material captures both the lower (SM11) and upper (SM4, SM14b) parts
476 of the Fordon Evaporite Fm.. In borehole SM11 (Figure 10), the lower part of the Fordon
477 Evaporite Fm. contained assemblages with a low yield. Palynomorphs were mostly of the
478 Unidentifiable type, corroded, dark and fragmented. However, some very well-preserved
479 specimens of *Illinites* sp., *Klausipollenites schaubergeri*, *Reduviasporonites* sp.,
480 *Lueckisporites virkkiae* Variant A and Variant B, and *Vestigisporites minutus* were recovered.

481       The upper part of the Fordon Evaporite Fm. in SM11 (Figure 10) contained a more
482 varied assemblage with samples containing greater yields. Very high proportions of
483 Unidentifiable pollen grains persisted, as well as some very well-preserved palynomorphs
484 originating in the evaporites. Assemblages were dominated by *Lueckisporites virkkiae* Variant
485 A, *Klausipollenites schaubergeri*, *Vestigisporites minutus* and assorted *Illinites* sp.,
486 *Taeniaesporites* sp. and *Protohaploxypinus* sp.

487       On average assemblages from the Fordon Evaporite Fm. from SM11 (Figure 10)
488 contained taeniate bisaccate species *Lueckisporites virkkiae* Variant A (13.3%), as well as
489 Variant B (4.1%) and Variant C (3.8%), *Taeniaesporites* sp. (5.2%), rare *T. angulistriatus*
490 (0.5%), *T. albertae* (1.3%), *T. noviaulensis* (1.0%), and *T. labdacus* (1.31%%), rare
491 *Protohaploxypinus* sp. (1.3%) including *P. chaloneri* (0.8%), *P. jacobii* (0.5%) and *P.*
492 *microcorpus* (0.5%). *Striatopodocarpites antiquus* (0.5%) and *Vittatina hiltonensis* (0.5%)
493 were very rare. The non-taeniate bisaccate pollen were represented by *Klausipollenites*
494 *schaubergeri* (6.4%), *Illinites* sp. (5.1%) including *I. delasaucei* (1.8%), and rare *Labiisporites*
495 *granulatus* (1.8%), *Falcisporites zapfei* (0.5%) and *Potonieisporites novicus* (0.5%).
496 Monosaccate pollen were rare and were represented by *Nuskoisporites dulhuntyi* (0.5%), yet
497 *Vestigisporites minutus* was abundant (6.7%). *Reduviasporonites* sp. was present (9.6%), yet
498 samples were dominated by Unidentifiable palynomorphs (74.52%). Some trisaccate pollen
499 grains were recovered (6.67%), as well as rare spores (0.5%) and very rare acritarchs (<0.5%).

500       The Unidentifiable component appears to increase in prominence throughout the upper
501 part of the Fordon Evaporite Fm. Species richness and abundance of palynomorphs also
502 appears to increase throughout the Fordon Evaporite Fm. as the proportion of Unidentifiable
503 palynomorphs progressively dominates samples.

504       Borehole SM4 (Figure 11) captures the top of the Fordon Evaporite Fm., where samples
505 either had a high yield or a very low yield (<100 pollen grains) yet were still dominated by
506 Unidentifiable palynomorphs (95.1%), which indicates pollen transport from a nearby source

vegetation. In addition to the Unidentifiable palynomorphs, rare *Lueckisporites virkkiae* (1.8 %) including Variant A (0.5%) and *L. virkkiae* Variant C (1.5%), *Taeniaesporites* sp. (4.3%), *Protohaploxypinus chaloneri* (1.5%), *Klausipollenites schaubergeri* (0.5%) and *Vittatina hiltonensis* (<0.5%), and unidentifiable spores (1.0%) were recovered. Only in the lower parts of the Fordon Evaporite Fm. were the three "Variants" of *L. virkkiae* distinguishable.

In borehole SM14b (Figure 12), the Fordon Evaporite Fm. palynomorph assemblages were generally well-preserved and of a high yield. Although containing a high proportion of Unidentifiable palynomorphs (80.0%), *Lueckisporites virkkiae* Variant A (11.0%) and Variant C (5%) are present, as well as *Klausipollenites schaubergeri* (5.9%), *Potonieisporites novicus* (7.0%) and *Illinites delasaucei* (7.0%), and *Reduviasporonites* sp. (3.0%). *L. virkkiae* Variant C was the latest variant to appear in the core relative to the other two.

*5.2.6. Cycle 2 – Cycle 3 transitional (EZ3 Ca) (grey salt clay/illitic shale/Grauer Salzton): SM4 borehole*

In SM4 (Figure 11) the Grauer Salzton/Brotherton Fm. boundary assemblage was dominated by Unidentifiable palynomorphs (87.7%), but unlike the other boreholes containing palynomorphs identifiable to species level the assemblage was found to contain *Lueckisporites virkkiae* Variant A (3.8%), Variant B (0.9%), and Variant C (2.8%), *Illinites* sp. (0.9%), *Labiisporites granulatus* (1.9%), *Taeniaesporites* sp. and *T. labdacus* (0.9%). In borehole SM7 (Figure 13) a single sample captures the palynology of the Grey Salt Clay. It contains an abundant assemblage composed only of Unidentifiable palynomorphs (100.0%). In borehole SM11 (Figure 10) this transitional stratum was either barren, or was composed of a very abundant sample of only 100.0% Unidentifiable palynomorphs. In SM14b (Figure 12) assemblages of the Grauer Salzton are barren.

*5.2.7. Cycle 3 carbonates (EZ3 Ca) (Brotherton Fm.): SM7, SM11 boreholes*

In borehole SM7 (Figure 13) a single assemblage from the Brotherton Fm. was recovered. Though of low yield (<200) the assemblage contains the taeniate bisaccate species *Lueckisporites virkkiae* (10.0%), including "Variants A" (2.5%), Variant B (1.0%) and very rare Variant C (0.5%). *Taeniaesporites* sp. (1.0%) was rare with *T. noviaulensis* (<0.5%) being very rare. *Protohaploxypinus* sp. was rare (<0.5%), *Illinites* sp. (1.5%) is present. *Klausipollenites schaubergeri* (8.0%) was present, *Vestigisporites minutus* was rare (0.5%) and was the only monosaccate species recovered. Well over half of the assemblage was composed of Unidentifiable palynomorphs (74.0%).

Many of the Brotherton Fm. samples from borehole SM11 (Figure 10) were barren (n=15). Recovered assemblages contain abundant palynomorphs, but were dominated by Unidentifiable palynomorphs (90.2%), presumably an effect of adverse preservational conditions during deposition. There appears to be an increase in the Unidentifiable component from the end of Cycle 2 evaporites through to the Brotherton Fm. However, not all samples were dominated by Unidentifiable palynomorphs. Some assemblages were very well-preserved.

Pollen taxa that occured in low abundances include the taeniate bisaccate species *Lueckisporites virkkiae* (4.8%) including abundant *L. virkkiae* Variant A (10.4%), with *L. virkkiae* Variant B (3.5%) and Variant C (1.3%), *Protohaploxypinus* sp. (3.3%), *Striatopodocarpites antiquus* (0.8%), *Taeniaesporites* spp. (2.0%) including *T. angulistriatus*

(0.5%), *T. noviaulensis* (0.5%), and *T. labdacus* (0.5%). Non-taeniate bisaccate pollen recovered were *Alisporites nuthallensis* (<0.5%), *Falcisporites zapfei* (<0.5%), *Illinites* sp. (3.3%) *I. klausi* (<0.5%) and *I. delasaucei* (0.5%), *Klausipollenites schaubergeri* (5.9%), *Labiisporites granulatus* (1.0%) and *Potonieisporites novicus* (<0.5%). The monosaccate pollen *Vestigisporites minutus* (7.8%), *Nuskoisporites* cf. *rotatus* (<0.5%), and *Nuskoisporites dulhuntyi* (<0.5%) were present. Trisaccate pollen grains and spores, and *Reduviasporonites* sp. were all rare (<0.5%).

The sample of Brotherton Fm. from SM4 (Figure 11) was barren. However, the sample of Brotherton Fm. from SM14b (Figure 12) contained an abundant yield of pollen, dominated by Unidentifiable palynomorphs (99.5%), but also contained very rare occurrences of *Lueckisporites virkkiae* (1.7%), and *Taeniaesporites* sp. (0.6%)


*5.2.8. Cycle 3 evaporites (Billingham Anhydrite (EZ3 A), Boulby Potash (EZ3 K) and Boulby Halite (EZ3 Na)): SM11 borehole*

Assemblages in borehole SM11 (Figure 10) became better-preserved throughout the evaporites, especially in the Billingham Anhydrite and Boulby Halite.


*5.2.9 Cycle 3 anhydrite (Billingham Anhydrite): SM11 borehole*

There was no recovery from the Billingham Anhydrite or lower part of the Boulby Halite in SM4 (Figure 11).

In SM11 (Figure 10) the Billingham Anhydrite assemblages yielded *Lueckisporites virkkiae* (7.5%), including Variant A (16.9%), Variant B (2.8%) and Variant C (3.5%), *Protohaploxypinus* sp. (1.3%), *P. chaloneri* (1.3%), *P. jacobii* (1.4%), *P. microcorpus* (0.9%) and *P.* cf. *samoilovichii* (0.5%), *Taeniaesporites* sp. (2.8%), *T. angulistriatus* (1.2%), *T. labdacus* (2.6%) and *T. novimundi* (1.5%) and *T. noviaulensis* (1.5%), *Striatopodocarpites* sp. (0.6%), *Striatoabieites antiquus* (1.6%) and rare *Vittatina hiltonensis* (<0.5%). Non-taeniate bisaccate pollen were represented by *Alisporites nuthallensis* (1.8%), *Falcisporites zapfei* (0.9%), *Illinites sp.* (5.0%), *I. delasaucei* (4.2%), *Klausipollenites schaubergeri* (16.3%), *Labiisporites granulatus* (1.5%), *Potonieisporites novicus* (0.8%). The multisaccate *Crustaesporites globosus* was present but rare (0.5%). The monosaccate pollen were represented by *Nuskoisporites dulhuntyi* (0.8%), *Perisaccus granulosus* (0.9%) and *Vestigisporites minutus* (6.3%). *Reduviasporonites* sp. (1.7%), spores (1.8%), and acritarchs (0.5%), were rare.


*5.2.10. Cycle 3 potassium-magnesium salts (Boulby Potash): SM11 borehole*

In SM11 (Figure 10) the Boulby Potash yielded an assemblage composed of the taeniate bisaccate species *Lueckisporites virkkiae* (49.5%), *Protohaploxypinus* sp. (0.5%), *P. jacobii* (2.5%), *P. microcorpus* (1.5%), *Taeniaesporites albertae* (2%), *T. labdacus* (2.5%) and *T. noviaulensis* (2.0%), the non-taeniate bisaccate species *Falcisporites zapfei* (1.0%), *Illinites tectus* (4.0%), *Klausipollenites schaubergeri* (4.5%), *Labiisporites granulatus* (18.0%), *Potonieisporites novicus* (0.5%), and the monosaccate species *Vestigisporites minutus* (5.0%) and *Perisaccus granulosus* (1.0%). *Reduviasporonites* sp. was present (5.0%), as well as very rare spores (<0.5%).

### 5.2.11. Cycle 3 halite (Boulby Halite): SM4, SM11 boreholes

In borehole SM11 (Figure 10) the Boulby Halite contained the taeniate bisaccate species *Lueckisporites virkkiae* (13.0%) including Variant A (21.7%), Variant B (1.4%) and Variant C (9.3%), *Protohaploxypinus* sp. (0.5%), including the species *P. chaloneri* (2.3%) and *P. jacobii* (2.5%), Taeniaesporites sp. (3.76%), *T. angulistriatus* (0.5%), *T. labdacus* (2.5%), the non-taeniate bisaccate species *Falcisporites zapfei* (1.0%), *Illinites* sp. (<0.5%), *Klausipollenites schaubergeri* (8.9%), *Labiisporites granulatus* (9.3%), *Potonieisporites novicus* (0.5%). The monosaccate pollen were represented by *Vestigisporites minutus* (6.2%) and *Perisaccus granulosus* (1.0%). *Reduviasporonites* sp. was present (2.6%) as well as very rare trisaccate species (<0.5%). The Unidentifiable component averaged at 58.7% of the assemblage.

In borehole SM4 (Figure 11) assemblages of Boulby Halite were either barren or contained assemblages of low yield, dominated on average 90.8% by Unidentifiable palynomorphs. *Klausipollenites schaubergeri* (8.7%), *Lueckisporites virkkiae* (11.0%), *Vestigisporites minutus* (2.9%), *Taeniaesporites* sp. (1.45%) including *T. novimundi* (2.9%) were recovered. It is in the Boulby Halite that *Vestigisporites minutus* makes its first appearance in borehole SM4, although earlier occurrences cannot be excluded on the basis of recovery of *V. minutus* in the Fordon Evaporite Fm. of borehole SM11.

### 5.2.12. Cycle 3 – Cycle 4 transition Carnallitic Marl Fm. (Rotten Marl): SM4, SM11 boreholes

Exceptionally well-preserved assemblages were extracted from the Carnallitic Marl Fm. in borehole SM11 (Figure 10) using standard palynological acid maceration techniques, representing the first time palynomorphs have been recorded from the formation.

In SM4 (Figure 11) an assemblage from the base of the Carnallitic Marl Fm. was not diverse or of high yield, but it was sufficiently well-preserved, relative to the underlying Boulby Halite, to recover *Lueckisporites virkkiae* (11.6%), *Klausipollenites schaubergeri* (8.7%), *Vestigisporites minutus* (9.2%), *Taeniaesporites* sp. (1.5%) including *Taeniaesporites novimundi* (2.9%), and Unidentifiable palynomorphs (72.5%)

Assemblages from the Carnallitic Marl Fm. of borehole SM11 (Figure 10) were of varying quality. Assemblages contained moderate amounts of Unidentifiable palynomorphs (15.3%) as well as distinctly well-preserved pollen grains. Taeniate bisaccate pollen were represented by the species *Lueckisporites virkkiae* (52.0%) including *L. virkkiae* Variant A (20.0%), *L. virkkiae* Variant B (4.4%), *L. virkkiae* Variant C (3.6%), *Protohaploxypinus* sp. (1.5%), *P. chaloneri* (1.7%), *P. jacobii* (0.8%), *Striatopodocarpites fusus* (<0.5%), *Taeniaesporites* sp. (3.0%), *T. albertae* (1.3%), *T. angulistriatus* (2.7%), *T. bilobus* (0.5%), *T. labdacus* (5.9%), *T. noviaulensis* (2.2%), *T. novimundi* (0.6%), and *Vittatina hiltonensis* (0.6%). Non-taeniate bisaccate pollen were represented by *Alisporites nuthallensis* (0.8%), *Falcisporites zapfei* (1.2%), *Illinites* sp. (3.0%), *I. delasaucei* (2.5%), *I. klausi* (0.5%), *I. tectus* (2.1%), *Klausipollenites schaubergeri* (11.4%), *Labiisporites granulatus* (0.8%), *Potonieisporites novicus* (0.5%). The multisaccate *Crustaesporites globosus* was present (1.0%). Monosaccate pollen were represented by *Nuskoisporites dulhuntyi* (<0.5%), *Perisaccus granulosus* (0.5%), and *Vestigisporites minutus* (5.1%). *Reduviasporonites* sp. (2.5%) and rare acritarchs (0.5%) were also present. The Carnallitic Marl Fm. in SM11 is the only recorded instance of *Taeniaesporites bilobus* in borehole SM11.

### 5.2.13. Cycle 4 carbonates (EZ4 Ca) Upgang Fm.: SM4, SM11 boreholes

In SM11 (Figure 10) the Upgang Fm. yielded assemblages composed of the taeniate species *Lueckisporites virkkiae* (52.0%), *Protohaploxypinus chaloneri* (0.5%), *P. jacobii* (<0.5%), *Taeniaesporites angulistriatus* (1.0%), *T. labdacus* (6.0%), *T. noviaulensis* (1.5%), *T. novimundi* (1.0%), *Striatoabieites richteri* (<0.5%), *Striatopodocarpites antiquus* (<0.5%), *Vittatina hiltonensis* (1.0%), and the non-taeniate bisaccate species *Falcisporites zapfei* (1%), *Illinites delasaucei* (2.0%), *Klausipollenites schaubergeri* (16.5%), *Labiisporites granulatus* (1.5%), *Potonieisporites novicus* (<0.5%). The monosaccate pollen were represented by *Perisaccus granulosus* (0.5%) and *Vestigisporites minutus* (9.0%). *Reduviasporonites* sp. (1.0%) was present but rare, and the Unidentifiable component was comparatively reduced (4.0%). The Upgang Fm. was not sampled in SM4 (Figure 11).

### 5.2.14. Cycle 4 evaporites (Sherburn Anhydrite (EZ4 A), Sneaton Halite (EZ4 Na) and Sneaton Potash (EZ4 K)): SM4, SM11 boreholes

Analysis of rock salt samples yielded palynological recovery from the Cycle 4 evaporites. Palynomorphs have not previously been recorded from either the Cycle 4 or Cycle 5 evaporites as they are not lithologies typically targeted for palynological analysis and are often missing from borehole cores as the underlying Carboniferous and earlier Permian strata are more commercially important. Therefore, the results presented here from Cycle 4 and above provide a unique insight into the vegetation during latest Zechstein times.

In SM11 (Figure 10) two samples from the lower Sneaton Halite, were of low yield and composed mostly of Unidentifiable pollen grains, however *Lueckisporites virkkiae* Variant C, *Klausipollenites schaubergeri*, and *Reduviasporonites* sp. were recovered as well. In SM11 one sample from the upper Sneaton Halite contained only rare Unidentifiable pollen (n=3).

In SM11 the Sherburn Anhydrite assemblage was dominated by Unidentifiable pollen grains (71.4%), and contained the taeniate bisaccate pollen *Lueckisporites virkkiae* (3.2%), *L. virkkiae* Variant C (9.4%), the non-taeniate bisaccate pollen *Klausipollenites schaubergeri* (1.6%), *Labiisporites granulatus* (9.1%), *Potonieisporites novicus* (9.1%), and considerable abundance of *Reduviasporonites* sp. (22.8%).

In borehole SM4 (Figure 11), the Sneaton Halite and Sneaton Potash assemblages did not have a high yield (<200 count) and are dominated by Unidentifiable palynomorphs (88.9-100.0%), though they contained *Klausipollenites schaubergeri* (7.4%) and *Lueckisporites virkkiae* (3.7%). The upper Sneaton Halite of borehole SM11 contained a single sample of very low yield composed only of Unidentifiable palynomorphs.

The Sneaton Potash in SM4 was dominated by Unidentifiable pollen grains (91.8%), with the assemblage also containing *Lueckisporites virkkiae* (8.2%) and *Klausipollenites schaubergeri* (8.5%).

### 5.2.15. Cycle 5 carbonates (EZ5 Ca) Sleights Siltstone: SM4 borehole

The Sleights Siltstone from borehole SM4 (Figure 11) contained an assemblage composed only of Unidentifiable palynomorphs at a very low yield (<200 count) (sample SM4 1258.63 m).

683

### 5.2.16. Cycle 5 evaporites (Littlebeck Anhydrite and Bröckelschiefer): SM11 borehole

There was no recovery from the Littlebeck Anhydrite in any of the borehole material. However, the Bröckelschiefer in SM11 (Figure 10) yielded an assemblage composed of *Lueckisporites virkkiae* Variant C (2.0%), *Illinites* sp. (5.0%) and dominated by Unidentifiable pollen grains (93.0%)

### 5.2.17. Latest Zechstein: Little Scar Beach outcrop

Samples from Little Scar (Figure 14) were mostly barren yet those that did contain a yield had a very low abundance of palynomorphs (<50). However, *Taeniaesporites* sp. was found in LSSC 1 (2.5%), and LSSC 1-6 did contain very low abundances of Unidentifiable palynomorphs (80.0-100.0%). LSSC 1 had the highest yield of palynomorphs at 38 palynomorphs per slide. What is most interesting about these samples is that LSSC 2 and LSSC 3 contained benthic foraminiferal test linings (Plate III, 10), which are indicative of relatively normal marine conditions. Foraminiferal test linings were incredibly rare throughout the material used in this study, only otherwise found in material from Salterford Farm borehole belonging to the Marl Slate (EZ1) (Plate III, 11). Belonging to Cycle 4-5, the strata at Little Scar beach form a useful comparison the strata of a younger age from Cycle 1.

### 5.3. Summary of the distribution of taxa within the stratigraphical sequence

### 5.3.1. Cycle 1 Marl Slate: the principal Zechstein transgression

The Marl Slate assemblages are generally very well preserved as they were recovered from bituminous anoxic shale. In terms of average percentage abundance, they are dominated by *Lueckisporites virkkiae* (53.5%) and *Taeniaesporites* spp. (22.5%), but also contain *Klausipollenites schaubergeri* (8.3%), *Illinites* sp. (5.5%), *Vestigisporites minutus* (5.5%), *Vittatina hiltonensis* (2.5%), and less than 2.0% each of *Alisporites nuthallensis*, *Crustaesporites globosus*, *Nuskoisporites dulhuntyi*, *Perisaccus granulosus*, *Protohaploxypinus* spp., *Striatopodocarpites* sp. and spores. In samples where Unidentifiable pollen grains are present, they represent 93.0% of the assemblage indicating poor preservation. Many pollen grains are of a hyaline nature making species identification difficult. Recovery of benthic coiled foraminiferal test linings from Salterford Farm borehole sample SF465 corroborates marine conditions during deposition.

### 5.3.2. Cycle 1 Carbonates

The Cycle 1 carbonates assemblages are generally more speciose than those from the Marl Slate and the palynomorphs are less hyaline in nature making species differentiation and identification easier. Assemblages are still dominated by *Lueckisporites virkkiae* (44.5%), but here the three variants of Clarke (1965) are distinguishable. *Klausipollenites schaubergeri* is more abundant than in the Marl Slate (13.7%) as well as *Illinites* sp. (5.5%) but with the three species *I. delasaucei*, *I. klausi* and *I. tectus* distinguishable, of which *I. delasaucei* reached abundances of 9.5%. *Vestigisporites minutus* is of similar abundance (4.8%) while *Vittatina hiltonensis* increased in abundance (3.2%). A variety of *Taeniaesporites* spp. are present

including *T. albertae* (5.5%), *T. angulistriatus* (1.7%), *T. labdacus* (4.5%), *T. noviaulensis* (3.0%) and *T. novimundi* (1.8%). *Alisporites nuthallensis* (2.4%) and *Labiisporites granulatus* (2.6%) increase in abundance. *Protohaploxypinus* sp. (0.6%), *P. jacobii* (1.3%), and *Falcisporites zapfei* (1.0%) are less abundant than in the Marl Slate, becoming rare, while *Nuskoisporites dulhuntyi* (0.5%), *Perisaccus granulosus* (0.5%), and *Striatopodocarpites* sp. (0.5%) maintain a rare abundance. *Striatoabieites richteri* (0.5%) and *Reduviasporonites* sp. (3.4%) appear, along with very rare tetrads (<0.5%). *Crustaesporites globosus*, *Cycadopites rarus* and acritarchs are not present. In the Cycle 1 carbonates better preservation enables the identification of more species, giving the impression of increased species richness. According to previous literature Zechstein Cycles 1 and 2 yielded the richest palynomorph assemblages, which this data supports, but a preservational bias should not be ignored.

### 5.3.3. Cycle 2 Carbonates

The Cycle 2 carbonate assemblages are also dominated by *Lueckisporites virkkiae* (53.5%), but only Variant A is distinguishable. *Alisporites nuthallensis* becomes rare (1.0%), *Illinites* sp. increases in abundance (8.4%), *I. delasaucei* decreases dramatically (<0.5%) and *I. klausi* and *I. tectus* disappeared. *Klausipollenites schaubergeri* (20.0%) and *Taeniaesporites* spp. (4.6%) increases in abundance yet fewer species are present with *T. noviaulensis* absent, and overall the abundance of individual species decreases, suggesting *Taeniaesporites* is not well enough preserved to distinguish species in these assemblages. *Protohaploxypinus* spp. continues to be rare (2.2%) however more species are present including *P. chaloneri* (0.5%), *P. jacobii* (<0.5%), and *P. microcorpus* (1.0%). *Nuskoisporites dulhuntyi* (1.0%) and *Perisaccus granulosus* (<0.5%) maintains a rare abundance. *Vestigisporites minutus* decreases in abundance by over a half (1.9%). *Falcisporites zapfei* (1.0%), *Vittatina hiltonensis* (0.5%), spores (<0.5%), *Striatopodocarpites* sp. (<0.5%) and *Potonieisporites novicus* (<0.5%) are rare. *Striatoabieites richteri*, *Platysaccus radialis*, and *Reduviasporonites* sp. disappears and *Crustaesporites globosus*, *Cycadopites rarus*, acritarchs, and tetrads are still absent. Unidentifiable pollen grains comprises on average 44.9% of assemblages, slightly less (~4.5%) than in the Cycle 1 carbonates.

### 5.3.4. Cycle 2 Evaporites

The Cycle 2 evaporite assemblages contains *Lueckisporites virkkiae* (5.5%) at much lower abundances but with all three variants distinguishable, due to a relative increase in the abundance of Unidentifiable pollen grains (77.4%), a result of many poorly preserved assemblages. Consequently, the abundance of many species appears to decline. *Illinites* sp. experiences a slight decline in abundance (5.6%) with *I. delasaucei* increasing in abundance (2.5%), and *I. klausi* reappearing (<0.5%) while *I. tectus* remains absent. *Klausipollenites schaubergeri* dramatically declines in abundance (6.4%), *Nuskoisporites dulhuntyi* declines (0.5%). *Protohaploxypinus* sp. is rare (1.3%), with little change in the species remaining from the Cycle 2 carbonates; *P. chaloneri* (1.5%), *P. jacobii* (0.5%), and *P. microcorpus* (0.5%). *Taeniaesporites* spp. overall experiences a slight increase in abundance (5.1%) and a reorganization of species as *T. noviaulensis* appears (1.0%) while *T. novimundi* disappears. *T. albertae* (1.3%) and *T. angulistriatus* (0.5%) maintain rare abundances. *Striatoabieites richteri* remains absent and *Striatopodocarpites* sp. disappears. *Vittatina hiltonensis* continues to be rare (<0.5%). *Alisporites nuthallensis* (1.0%) as well as *Perisaccus granulosus* (0.5%) maintain low abundances. *Falcisporites zapfei* disappears. However, some species experience increases in abundance such as *Labiisporites granulatus* (1.8%), *Nuskoisporites* cf. *rotatus* appears for

the first time (<0.5%), *Platysaccus radialis* reappears but is very rare (<0.5%), *Potonieisporites novicus* increases slightly in abundance (2.6%). *Reduviasporonites* sp. reappears at considerable abundance (8.4%). *Cycadopites rarus*, acritarchs and tetrads remain absent while spores maintain a rare abundance (0.8%).

### 5.3.5. Cycle 3 Carbonates

The Cycle 3 carbonate assemblages display a continuing trend of increasingly abundant Unidentifiable pollen grains (89.1%) at the expense of identifiable species. *Lueckisporites virkkiae* is present at yet again slightly lower abundances (4.5%), however all variants are distinguishable. *Alisporites nuthallensis* becomes very rare (<0.5%). *Illinites* sp. declines again in abundance (3.1%), along with *I. delasaucei* (0.5%), while *I. tectus* maintains its very rare abundance (<0.5%). *Klausipollenites schaubergeri* continues to decline (5.9%), as does *Labiisporites granulatus* (1.5%). *Nuskoisporites* cf. *rotatus* (<0.5%), *N. dulhuntyi* (<0.5%), and *Potonieisporites novicus* (0.5%) maintain rarity. No individual species of *Protohaploxypinus* are distinguishable, and *Protohaploxypinus* sp. maintains rarity (1.0%). *Reduviasporonites* sp. dramatically decreases from 8.8% to extremely rare (<0.5%). *Taeniaesporites* spp. experiences a considerable decrease in abundance (1.6%) with *T. labdacus* (0.7%), *T. noviaulensis* (1.0%) and *T. angulistriatus* remaining rare (1.0%). *Vestigisporites minutus* decreases further in abundance (3.2%). *Striatoabieites richteri* remains absent, *Perisaccus granulosus*, *Platysaccus radialis* and *Vittatina hiltonensis* are not present. However, *Striatopodocarpites antiquus* reappears but is rare (0.5%) alongside *Falcisporites zapfei* (<0.5%). Trisaccate pollen grains are very rare (<0.5%).

### 5.3.6. Cycle 3 Evaporites

In the Cycle 3 evaporites many species experience an increase in abundance accompanied by a decline in the proportion of Unidentifiable pollen grains (60.9%). *Alisporites nuthallensis* maintains rarity (1.8%), *Crustaesporites globosus* reappears but is rare (<0.5%), *Cycadopites rarus* occurs for the only time in the Zechstein succession (0.5%), *Falcisporites zapfei* maintains rarity (0.9%). *Illinites* sp. increases (5.0%) and *I. delasaucei* (4.2%) and *I. tectus* (5.2%) experience large increases, while *I. klausi* is absent. The abundance of *Klausipollenites schaubergeri* returns to Cycle 2 levels (14.1%), and *Labiisporites granulatus* also recovers (5.1%). *Lueckisporites virkkiae* also starts to recover but does not reach early Zechstein abundances (8.9%), however all three variants are distinguishable, with Variant A notably accounting for 18.6% of assemblages. *Nuskoisporites dulhuntyi* is still rare (0.8%) as well as *Potonieisporites novicus* (0.9%), and *Perisaccus granulosus* reappears (0.9%). All species of *Protohaploxypinus* are present with undifferentiated individuals only comprising 1.1% of assemblages. *P.* cf. *samoilovichii* (0.5%), *P. chaloneri* (1.5%), *P. jacobii* (1.7%), and *P. microcorpus* (1.1%) reappear. *Reduviasporonites* sp. increases slightly (1.8%), *Striatopodocarpites antiquus* is still rare (1.2%) and *Striatopodocarpites* sp. reappears (1.1%). *Taeniaesporites* sp. increases (2.9%) and *T. alb*ertae (2.0%) and *T. novimundi* (1.7%) reappear, while *T. angulistriatus* maintains low abundance (1.1%). *T. labdacus* (2.6%) and *T. noviaulensis* (1.8%) both increase marginally in abundance. *Vestigisporites minutus* increases in abundance (5.9%), *Vittatina hiltonensis* reappears although is very rare (<0.5%). However, some species do not recover. *Nuskoisporites* cf. *rotatus* is absent. *Platysaccus radialis* and *Striatoabieites richteri* remain absent, as do tetrads. However, acritarchs (0.5%) and trisaccate pollen grains (0.5%) were recovered although no spores were recovered.

### 5.3.7. Cycle 4 Carbonates

The Cycle 4 carbonate assemblages are once again dominated by *Lueckisporites virkkiae* (52.0%), with all three variants distinguishable. The Unidentifiable component is considerably reduced (13.9%). Other species also experience increases in abundance. *Crustaesporites globosus* increases slightly (1.0%). *Nuskoisporites* cf. *rotatus* reappears (1.0%) however, *N. dulhuntyi* decreases slightly (0.5%). *Platysaccus radialis* reappears at very rare abundances (<0.5%). *Striatoabieites richteri* reappears and *Striatopodocarpites fusus* appears for the first time, both at very rare abundances (<0.5%). *Taeniaesporites* sp. increases slightly (3.0%), with increases also seen in *T. angulistriatus* (2.3%), and *T. labdacus* (5.9%). *T. bilobus* appears for the first and only time (0.5%). *T. albertae* (1.3%), *T. noviaulensis* (0.7%) and *T. novimundi* (0.7%) maintain their rarity alongside *Vittatina hiltonensis* (0.7%). *Vestigisporites minutus* more or less maintains abundance (5.6%). Other species experience noticeable reductions. *Klausipollenites schaubergeri* declines slightly in abundance (12.1%), *Alisporites nuthallensis* maintains low abundance (0.5%), while *Illinites* sp. reduces slightly (3.0%), with slight decreases in *I. delasaucei* (2.4%) and *I. tectus* (2.0%), while *I. klausi* reappears at low abundances (0.5%). *Perisaccus granulosus* (0.5%) and *Potonieisporites novicus* (0.5%) maintain rare abundances. *Protohaploxypinus* sp. (1.5%) is present at low abundance within individual species also occurring at low abundance or being rare; *P. chaloneri* (1.4%), *P. jacobii* (0.9%) and *P. microcorpus* (0.5%). *Reduviasporonites* sp. declines slightly (1.8%), *Striatopodocarpites antiquus* disappears. *Cycadopites rarus* and *Striatopodocarpites* sp. are absent. Acritarchs maintain a rare abundance (0.5%), while tetrads and spores remain absent. No trisaccate pollen grains are recovered after the Cycle 4 carbonates.

### 5.3.8. Cycle 4 evaporites and Cycle 5

The assemblages from Cycle 5 carbonates and evaporites are comparatively impoverished with samples having low yields, a trend that appears to start in the Cycle 4 evaporites. The Cycle 4 evaporites contain an assemblage dominated by Unidentifiable pollen grains (84.2%), accompanied by the fungus/algae *Reduviasporonites* sp. (22.8%), *Lueckisporites virkkiae* (15.7%), *Protohaploxypinus* cf. *samoilovichii* (9.1%), and *Klausipollenites schaubergeri* (5.8%). In the Cycle 5 carbonates only Unidentifiable pollen grains (96.0%) were recovered from borehole material, and benthic coiled foraminiferal test linings (15.0%) from outcrop at Little Scar Beach (samples LSSC 2 and LSSC3). The Cycle 5 evaporites from borehole material only contain sparse *Illinites* sp. (5.0%), *Lueckisporites virkkiae* (2.0%) and an abundance of Unidentifiable pollen grains (93.0%).

### 5.4. Comparison of the Durham and Yorkshire Sub-basins

Comparisons between spore-pollen assemblages from the Yorkshire and Durham Sub-basins are only possible for the lower cycles as the upper cycles from the Durham Sub-basin have not yielded palynomorphs.

In terms of the lowest cycle Cycle 1 The Marl Slate/'Lower Magnesian Limestone' assemblages in Salterford Farm borehole (Yorkshire Sub-basin) contain more taxa than Claxheugh Rock and Crime Rigg Quarry (Durham Sub-basin). However, differences are likely the result of differential preservation as the proportion of Unidentifiable pollen grains is

864 considerably lower in Salterford Farm compared to the samples from Claxheugh Rock and
865 Crime Rigg Quarry, and in general samples from the Marl Slate of the Durham Sub-basin are
866 more hyaline in appearance than those from the Yorkshire Sub-basin. *Illinites delasaucei,*
867 *Klausipollenites schaubergeri, Lueckisporites virkkiae* Variant A, *Vestigisporites minutus* are
868 the most common species in Salterford Farm. *Lueckisporites virkkiae, Taeniaesporites* spp.,
869 *Illinites* spp., *Vestigisporites minutus* and *Klausipollenites schaubergeri* are most abundant
870 taxa in Claxheugh Rock, and *Illinites* spp., *Klausipollenites schaubergeri, L. virkkiae,*
871 *Taeniaesporites* spp. and *Vestigisporites minutus* are the most common species in Crime Rigg
872 Quarry. In addition, *Taeniaesporites* spp. is more abundant in the Durham Sub-basin. It appears
873 that *Vestigisporites minutus* is not a common component of early Zechstein palynofloras. *V.*
874 *minutus* is present in low abundance at Kimberley and in Woolsthorpe Bridge borehole, but
875 maintains considerable presence through the Salterford Farm borehole. In the Durham Sub-
876 basin *V. minutus* is only present in one sample from Claxheugh Rock yet is reasonably
877 abundant in the single sample from Crime Rigg Quarry.

878 The Cadeby Formation exposed in the Kimberley railway cutting, that was
879 palynologically analysed by Clarke (1965), was resampled. The assemblages described here
880 correspond to samples K5 and K6 of the original study. Our findings are very similar to those
881 of Clarke (1965), but with some minor differences that concern observations on taxa that are
882 rare in the assemblages. Our study did not recover *Striatopodocarpites cancellatus* or
883 *Labiisporites granulatus.* The reprocessed K5 sample revealed the presence of *Taeniaesporites*
884 *angulistriatus, Striatopodocarpites antiquus, Vittatina hiltonensis, Illinites tectus, Perisaccus*
885 *granulosus, Nuskoisporites dulhuntyi, Potonieisporites novicus* and *Alisporites nuthallensis.*
886 Both the original study and this study note the absence of *Vestigisporites minutus*, a species
887 that is abundant throughout the borehole and outcrop material. *Alisporites nuthallensis* was
888 identified in this analysis of the Kimberley material and different *Protohaploxypinus* species
889 were identified in Clarke's study. These two genera are both rare meaning any disparity in
890 presence and abundance is likely due to the rarity of these two taxa and the low probability of
891 all species occurring in all of the slides made from the same sample.

892 Previous work on the Cycle 1 carbonates from Woolsthorpe Bridge (Warrington, 1980;
893 Berridge et al., 1999) recorded the presence of a characteristic Zechstein miospore assemblage
894 composed of *Alisporites* sp., *Crustaesporites* cf. *globosus, Falcisporites zapfei,*
895 *Klausipollenites schaubergeri, Lueckisporites virkkiae,* ?*Perisaccus granulosus,*
896 *Protohaploxypinus* spp., *P.* cf. *chaloneri, P.* cf. *jacobii, P. microcorpus,* ?*Striatopodocarpites*
897 sp., *Taeniaesporites* spp., *T. labdacus, T. noviaulensis. Labiisporites granulatus,*
898 *Taeniaesporites albertae,* and *Vestigisporites minutus* were not recorded (G. Warrington pers.
899 comm.) but have been recovered during this study.

900 Recovery of an assemblage from the Cadeby Formation, comparable to those from the
901 'Lower Marl' at Kimberley, Cinderhill, and Woolsthorpe Bridge, has previously been reported
902 from Salterford Farm (Warrington, 1980; Berridge et al., 1999). The age of these assemblages
903 has been interpreted as Lopingian based on the presence of *Lueckisporites virkkiae.*

904

905 *6. Reconstructing the Zechstein flora*

906 *6.1. General comments: palaeoecology*

907 The Zechstein Sea was located within the Permian Euramerican phytogeographical
908 province with a flora dominated by abundant conifers and pteridosperms with rare
909 ginkgophytes, sphenophytes, ferns, lycopsids and potentially cycads (Schweitzer 1986; Cleal

and Thomas, 1995). Detailed descriptions of Lopingian Euramerican flora have been provided for England, Germany and Poland (e.g. Kurtze, 1839; Geinitz, 1869; Solms-Laubach, 1884; Gothan and Nagelhard, 1923; Weigelt, 1928, 1930; Stoneley, 1958; Schweitzer, 1960, 1962, 1968, 1986; Ullrich, 1964; Poort and Kerp, 1990; Brandt, 1997; Uhl and Kerp, 2002), Spain (Bercovici et al., 2009), and the southern Alps (e.g. Clement-Westerhof, 1984, 1987, 1988; Visscher, 1986; Kutstatcher et al., 2012, 2014, 2017; Labandiera et al., 2016). A Zechstein-type flora has also been reported from Belgium (Florin, 1954). The floras are generally found in deposits of marginal marine or fluvial lowstand settings (e.g., Ullrich, 1964, Weigelt, 1928; Weigelt, 1930; Schweitzer, 1968; Schweitzer, 1986; Uhl and Kerp, 2002). It appears that the vegetation was fairly uniform across the basin, low in diversity and dominated by conifers (see Table 2), suggesting an arid to semi-arid environment and with plants adapted to periodic water stress.

The British Zechstein flora has been described in detail by Stoneley (1958) and Schweitzer (1986). Due to the suggested Lopingian climate trend towards increasing aridification the Zechstein flora has been interpreted as most abundant during Cycle 1 and the principal transgression and gradually disappearing from Cycle 2 onwards (Schweitzer, 1986). A similar trend of gradual decline was also suggested based on previous interpretation of palynomorph assemblages (Pattison et al., 1973; Smith et al., 1974).

Botanically based climatic inferences can be made from anatomical structures or by comparisons with other similar Lopingian Euramerican floras. The conifers and peltasperms from the Zechstein Basin and southern Europe exhibit some xerophorphic adaptations. They have very thick papillate cuticles, deeply sunken stomata, stomatal pores covered by overarching papillae, and some conifers leaves seem to have been thick and fleshy. However, not all taxa in the plant assemblages are fully adapted to xerophytic conditions.

The British Zechstein flora was previously divided into two groups based on their palaeoecology (Schweitzer, 1986). A xerophytic *Callipteris*-conifer association, which corresponds to the *Callipteris-Walchia* association of Gothan and Gimm (1930), and a hygrophylic *Neocalamites*-Sphenopterid association that corresponds to the *Calamites*-pecopterid (fern) association of Gothan and Gimm (1930). However, given more recent reconstructions of Lopingian Euramerican vegetation (e.g., Bercovici et al., 2009; Kutstatcher et al., 2012, 2014; Labandiera et al., 2016; Kustatscher et al., 2017) a different structure is proposed. It is likely that conifers (e.g., *Ullmannia*, *Pseudovoltzia*, *Ortesia*) with their more xerophytic adaptations occupied the arid to semi-arid, well-drained, inland and hinterland areas and low-lying slopes of the Protopennines. Pteridosperms (peltasperms) (e.g., *Peltaspermum*) with their thicker cuticles likely inhabited coastal areas, living in drier lowland patches, and in the hinterlands with the conifers. Horsetails (*Neocalamites*) likely occupied wet lowland riparian environments, shallow water coastal bogs and lakes, and the mouth of rivers. Pteridosperms (e.g. *Sphenopteris*) likely inhabited slightly less humid habitats while ginkgophytes (e.g. *Sphenobaieria*) and potential cycads (e.g. *Pseudoctenis*, *Taeniopteris*) inhabited more humid lowland areas near bodies of water.

The dominance of taeniate bisaccate pollen of conifer and pteridosperm affinity in this study concurs with previous investigations. While their dominance in assemblages likely reflects the general nature of the parent vegetation, it should be noted that multitaeniate pollen grains were produced by multiple plant groups (Chaloner, 2013), and there may also be a taphonomic bias towards bisaccate pollen due to their thick exines. Pollen grains of probable ginkgo and possible cycad (*Cycadopites rarus*) affinity are rare. This is expected as ginkgophytes are known to be rare components of the Zechstein flora, with some exceptions (e.g. Bauer et al. 2014), and potential cycads even rarer. However, this may also be the result

958　of a taphonomic bias. Finally, interpreting the exact nature and habitat of the vegetation is also
959　complicated by the lack of autochthonous plant remains beyond Cycle 1.

960

961　*6.2. Vegetation change through time*

962　　　　The changing nature of spore-pollen assemblages through the Zechstein sequences of
963　northeast England, as reported in this study, can be interpreted to document the changing nature
964　of the flora. The affinities of many of the spore-pollen taxa are well documented. However, in
965　some cases the lack of in situ occurrences means that some abundant bisaccate taxa, such as
966　*Labiisporites granulatus*, and some monosaccate pollen taxa, such as *Vestigisporites minutus*
967　and *Perisaccus granulosus*, have not yet been assigned to a parent plant group.

968　　　　The palynological data spans almost the entire temporal extent of the Zechstein,
969　allowing a reinterpretation of the flora. Plants were assumed to gradually disappear after Cycle
970　2 due to aridification and high rates of evaporation, with aridity being enhanced by the
971　decreasing magnitude of successive transgressive episodes. Instead, the assemblages from the
972　upper Zechstein Cycle 4 and Cycle 5 show that the conifer-pteridosperm dominated flora
973　persisted through to the Permian-Triassic boundary. This was likely facilitated by increasing
974　fluvial activity, seen in the increase in terrigenous fluvial sediments, from the end of Cycle 3
975　onwards. Presumably, this provided sufficient humidity to support the flora. Thus, it appears
976　likely that the flora had an azonal distribution that was more severely influenced by edaphic
977　factors than larger scale climate change.

978　　　　While the upper Zechstein (Cycle 4-5) assemblages suggest a decline in the flora
979　towards the Permian-Triassic boundary this may also be a taphonomic effect. The assemblages
980　recovered from the Carnallitic Marl Formation (Cycle 4) in SM11 (Figure 10) and SM4 (Figure
981　11) yield palynomorph assemblages of similar composition and abundance to those recovered
982　from the Marl Slate (Cycle 1) (Figure 4-6), suggesting that conditions were not as inhospitable
983　during the upper Zechstein as previously assumed.

984　　　　In the British Isles the Zechstein can be divided either into the classic five carbonate-
985　evaporites cycles or seven evaporite-carbonate sequences based on Tucker's (1991) sequence
986　stratigraphic scheme for the basin margins. The pollen charts in Figures 4-14 have been
987　presented against both organisations. The sequence stratigraphic approach is particularly
988　appropriate as the locations studied here are marginal marine. Changing shorelines would have
989　had significant impacts on the Zechstein vegetation, with highstands and lowstands effecting
990　groundwater levels, precipitation, and therefore the distribution of suitable wetter habitats and
991　taphonomic windows. Interpreting the data at the scale of transgression-regression cycles or
992　sequences may reveal the responses of vegetation to the accompanying patterns of drastic
993　climatic and environmental changes.

994　　　　Long term changes across the Zechstein sequence and slow rates of change are likely a
995　reflection of climate and environmental trends of increasing aridity and temperature that
996　characterise the Lopingian. The Zechstein Group covers the last ~6 million years of the
997　Permian meaning any slow changes may be indicative of floral turnover associated with the
998　end-Permian mass extinction. While the assemblages of Cycle 5 are comparatively
999　impoverished and composed of highly degraded Unidentifiable pollen grains, this may also be
1000　indicative of longer, water-borne transport from inland or hinterland areas via the fluvial
1001　depositional system of Cycle 5 instead of reflecting the true nature of the state of the flora.
1002　Furthermore, there is no coincident increase in spores with the reduction in Cycle 5

assemblages that typifies the floral turnover at the Permian-Triassic boundary. Yet, this may also be a taphonomic effect since assemblages are generally poorly preserved.

The cyclic transgressions into the Zechstein Basin would have forced the hydrological cycle by shifting coastlines and altering local topography. During highstands increased runoff likely caused high groundwater stages in lowland areas already characterised by more hygrophytic flora. During lowstands reduced runoff may have led to increased drainage and desiccation of lowlands with the low-lying Protopennines already characterised by more xerophytic flora. This can explain coeval occurrences of wet and dry lowlands and intrazonal vegetation throughout the Zechstein. Palynological assemblages may be expected to reflect these changing conditions, yet this is not necessarily reflected in the results presented here.

Ginkgophytes, horsetails ferns, lycopsids and possible cycads are among the rarest elements in the Zechstein flora, living around lakes and abandoned river channels, or along streams in a distal flood plain setting. While this is supported by their relative absence in the microfossil record, and may reflect the true nature of the vegetation, it may also be a taphonomic effect. Their dependence on the vicinity of large bodies of water or elevated ground water levels would have made them more sensitive to changes in sea level accompanying the Zechstein cycles.

The magnitude of sea level change diminished with each cycle as the sea progressively shrank in volume. The hygrophytic flora would have become increasingly stressed by the restriction of its habitat and the diminishing taphonomic window resulting in their rarity in the fossil record as both micro- and macrofossils. While their absence may be explained by sparsely distributed wet habitats suitable for reproduction, e.g., bryophytes are dependent on moist substrate upon which to reproduce (Whitaker and Edwards, 2010), it may reflect the poor preservation potential of certain palynomorph morphologies relative to the thicker walled conifer and pteridosperm bisaccate pollen. For example, horsetails are known to thrive in disturbed, anoxic, and saline environments (Husby, 2013) making them ideally suited to coastal Zechstein environments. Therefore, the rarity of horsetails in the microfossil record may be explained by the poor preservation potential of their palynomorphs. Modern horsetails (*Equisetum*) produce spores that are enveloped by four flexible ribbon-like elaters that are incredibly fragile (Marmottant et al., 2013). Furthermore, horsetails have a remarkable ability to reproduce vegetatively via rhizomes, compensating for the inefficiency of reproduction via spores, allowing horsetails to rapidly colonize coastal environments (Hauke, 1963), whilst remaining under-represented in the microfossil record.

Sea level highstands may explain the preferential preservation of coastal, nearshore, and inland habitats in certain strata, for example the Marl Slate (Cycle 1 transgression) and Carnallitic Marl Fm. (Cycle 3-4 boundary). Both are known for an abundance of microfossil remains, with the Marl Slate being notable for its macrofossil remains due to favourable taphonomic conditions. Increasing energy levels during the initial Zechstein transgression caused by the middle Wuchiapingian sea level highstand (Legler et al., 2011; Legler and Schneider, 2013) led to the rapid burial of material and the movement of azonal, coastal, flora into the taphonomic window created by this marginal environment. The transgression also established a distal fluvial plain with meandering and abandoned channels (like those at Pot Riding, Cadeby Formation, Cycle 1), resulting in the impression of a richer and lusher vegetation (e.g. Kustatscher et al., 2017). The Carnallitic Marl Fm. marks the initiation of a humid fluvial environment and therefore is also affected by a similar favourable taphonomic bias. With higher sedimentation rates the preservation potential of the Marl Slate and Carnallitic Marl Fm. was considerably higher than that of other sedimentary settings resulting in a higher local diversity relative to other palynomorphs assemblages.

Unfortunately, the scarcity of plant macrofossils from beyond Cycle 1 means it is not possible to investigate the effects of sea level change on macrofossil preservation in the upper Zechstein, when sea level changes were of a lesser magnitude relative to the lower Zechstein, e.g., 1-2 meters rather than the sea level drop of 100-150m between Cycle 1 and Cycle 2 (Smith, 1989). The absence of the Cycle 1 evaporites (Hayton Anhydrite/Hartlepool Anhydrite) means there is no palynological data for the first major regression and evaporative phase and the biotic responses of the flora cannot be reconstructed. By Cycle 2 the vegetation had already experienced a drastic environmental transition between arid and marine-buffered conditions during the evaporative phase of Cycle 1.

There are several possible trends discernible from the Zechstein palynoflora. There appears to be an overall reduction in palynomorph diversity and abundance through the Zechstein Group, punctuated by taphonomic effects. *Lueckisporites virkkiae* consistently dominates assemblages by up to ~50.0%. It is a typical Zechstein taxon recovered in the Baltic (Podoba, 1975), throughout Europe (e.g. Klaus, 1963; Clarke, 1965; Visscher, 1971; Massari et al., 1988; Warrington and Scrivener, 1988; Massari et al., 1994, 1999; Pittau, 1999; Legler et al., 2005; Pittau, 2005; Legler and Schneider, 2008; Warrington, 2005, 2008; Gibson et al., 2020) and from age equivalent deposits in the U.S.A. (Wilson, 1962; Clapham, 1970). It is an important and distinct conifer signal throughout the Zechstein.

The Marl Slate palynoflora is abundant, corroborating previous studies of taxonomic diversity and relative abundance of palynomorph taxa, mirroring previous reports of the macrofossil record (Stoneley, 1958; Schweitzer, 1986). At the top of the Cycle 2 Fordon Evaporite Fm. there appears to be an increase in pollen abundance seen in SM4 (Figure 11) and SM11 (Figure 10). In particular, Unidentifiable pollen increase in abundance approaching the Cycle 2-3 boundary. This may be in response to increasing sea level during the late regressive-early transgressive phase expanding the distribution of coastal habitats and the taphonomic window. This trend is also visible in SM14b (Figure 13) where Unidentifiable pollen grains increase over the Cycle 2-3 boundary and the number of taxa present decline across the Grauer Salzton into the Brotherton Fm. *Lueckisporites virkkiae* and *Taeniaesporites* spp. survive the boundary, and *Nuskoisporites* appears. Before the boundary, an assemblage of *Illinites delasaucei*, *Klausipollenites schaubergeri*, *Labiisporites granulatus*, *Lueckisporites virkkiae*, *Potonieisporites novicus*, *Reduviasporonites*, *Taeniaesporites* sp. and *Vestigisporites minutus* is present. It would appear a strong taphonomic bias is in effect as Unidentifiable pollen grains come to utterly dominate assemblages throughout the Brotherton Fm.

Preservation within the Cycle 3 evaporites (Billingham Anhydrite) of SM11 (Figure 10) is exceptional and the intermittent recovery throughout the evaporites is related to a lower sampling resolution through the evaporites instead of barren samples. The Carnallitic Marl Fm. palynoflora provides unique inside into the Cycle 3-Cycle 4 boundary flora. There is a noticeable increase in identifiable pollen species over the boundary. The assemblages recovered from the Carnallitic Marl Fm. from SM4 and SM11 (Figures 10-11) illustrate how conifers represent the most dominant component of the vegetation in the upper Zechstein e.g., *Lueckisporites virkkiae*, *Taeniaesporites* sp., and *Illinites* sp. Pollen grains of probably pteridosperm affinity occur less frequently e.g. *Protohaploxypinus* sp., *Striatoabieites* sp., *Striatopodocarpites* sp. and *Vittatina hiltonensis*. Throughout Cycle 4 some species disappear including *Vittatina* sp. (*Vittatina hiltonensis*) (Plate II, 1, 2). It is known to be rare in Lopingian assemblages (Clarke, 1965; Variakhuna, 1971) yet it appears intermittently though boreholes SM4 (Figure 11) an SM11 (Figure 10), at abundances no greater than 1.0%, until the Cycle 4 carbonates after which it disappears.

SM11 (Figure 10) has the longest temporal range of all boreholes studied and provides the best insight into the uppermost Zechstein flora. Palynomorphs were recovered across the Carnallitic Marl Fm.-Sleights Siltstone-Littlebeck Anhydrite boundaries, but then tail off and only Unidentifiable pollen grains are recovered through the rest of the sequence. The upper Zechstein trends are heavily affected by sampling resolution and the effect of the depositional settings on the quality of preservation. The relative proportions of conifer and pteridosperm pollen does not shift with conifer pollen being consistently more abundant. This trend continues into the uppermost Zechstein, with the recovery of *Illinites* spp. from the Little Scar assemblages, confirming the dominance of conifers throughout the Zechstein.

The palynflora does not suggest evidence of vegetation destabilisation which is associated with the end-Permian mass extinction (Looy et al., 2001; Lindström and McLoughlin, 2007; Hochuli et al., 2010; Xiong and Wang, 2011; Hochuli et al., 2016; Schneebeli-Hermann et al., 2017; Fielding et al., 2019; Novak et al., 2019). Instead it suggests an azonal vegetation dominated by conifers and pteridosperms inhabited a semi-arid landscape up to the Permian-Triassic boundary.


## 7. Palynofacies and the Zechstein palaeoenvironments

The fossil record is a result of the complex interplay between biotic and abiotic factors, and the composition of each palynomorph association is controlled by ecological factors, the depositional environment and taphonomic processes. Therefore, disentangling preservational biases from biological signals is vital for palaeoecological reconstructions. Zechstein spore-pollen assemblages are a case in point.

The Zechstein Group is interpreted as mostly marine in origin, albeit rather unusual due to varying and increased salinity related to the evaporation-replenishment cyclicity, with the upper Zechstein (Cycles 4-5) recognised as predominantly fluvial-terrestrial. However, the paucity of marine palynomorphs remains surprising for the lower Zechstein (Cycles 1-3). The palynomorph assemblages are entirely dominated by allochthonous forms derived from the adjacent land mass: pollen, spores, and land plant cuticles (Stoneley, 1958). Presumably, these were transported in from the land by a combination of wind and water. The latter was probably most significant during siliciclastic phases of sedimentation and surely must have been the principal transporter of large fragments of plant cuticle. The former may, however, have been important in transporting pollen into hypersaline pools from which the evaporites were deposited. Acritarchs, indicative of marine influence, are surprisingly rare. They are absent from most samples despite sieving at 10μm and, where present, constitute no more than 0.5% of assemblages. In this study we only report *Micrystridium*-type from Cycle 3 evaporites and Cycle 4 carbonates, although Wall and Downie (1963) previously reported them from Cycle 1 only. The lack of acritarchs presumably reflects the harsh hypersaline marginal conditions that were not conducive for marine phytoplankton to thrive.

The rare foraminiferal test linings from Salterford Farm and Little Scar beach are of interest both for their rarity and location in the stratigraphic column, specifically for the specimens recovered from Little Scar. These may represent the latest occurrence of Permian foraminifera recovered in the UK (B. Spencer pers. comm.). Encrusting foraminifera have been well-documented from the Polish Zechstein reef systems (Peryt et al., 2012) where they form important constituents of the limestone formations during the early Zechstein. These test linings are benthic coiled forms, but their low quality of preservation makes taxonomic identifications difficult. The foraminifera from Salterford Farm are not unexpected as the sea during Marl Slate times was representative of relatively normal shallow marine conditions.

However, from Little Scar, close to the Permian-Triassic boundary, benthic foraminifera appear in sediments interpreted as accumulating in the arid and hypersaline environments of the later Zechstein cycles.

*Reduviasporonites* in the British Permian has been correlated with brackish environments (Warrington, 2008). This is compatible with the pattern of recovery of these palynomorphs in this study. This reconstruction suggests that pockets of wetter environment persisted throughout the Zechstein. A fungal affinity has been invoked for *Reduviasporonites* with it interpreted as a saprophytic agent responsible for the degradation of widespread abundant dead organic matter preceding the end-Permian mass extinction (Visscher et al., 1996, 2011; Hochuli, 2016). Mass occurrences of *Reduviasporonites* have been interpreted as an end-Permian fungal spike, coincident with vegetation die-off and environmental disturbance prior to and during the extinction. However, high abundances of *Reduviasporonites* have also been attributed to 'algal blooms' (Elsik, 1999; Afonin et al., 2001; Foster et al., 2002; Spina et al., 2015). Regardless of affinity, mass occurrences of *Reduviasporonites* are an important stratigraphical marker of the Permian-Triassic boundary in terrestrial and shallow marine environments. Interestingly, *Reduviasporonites* maintains a rare to low abundance throughout the Zechstein sequence, but occurs at higher abundances at the top of the Fordon Evaporite Fm. (8.4%) (Cycle 2 (EZ3 A, K-Mg, Na) and in the Cycle 4 evaporites (Sherburn Anhydrite, Sneaton Halite) (22.8%). However, recovery at this high abundance was only recorded in one sample of <100 yield (see Table 1 Appendix B and Appendix E SM11 1478.30 m) which is not conclusive evidence of a mass occurrence. The lack of a definitive "spike" in abundance at the top of the Zechstein sequence may be viewed as further evidence that there was no significant deforestation or vegetation turnover during Zechstein times.

A variety in quality of preservation is observed in the Zechstein material: (i) assemblages dominated by beautifully preserved palynomorphs of low thermal maturity (e.g. from the Marl Slate); (ii) assemblages dominated by very well-preserved palynomorphs that are dark in colour. (e.g. from the Carnallitic Marl Fm in SM11 Dove's Nest); (iii) assemblages dominated by AOM but containing well-preserved yet hyaline palynomorphs which need to be stained with Bismarck Brown to facilitate identification (e.g. from the Marl Slate at Claxheugh Rock); (iv) assemblages of abundant Unidentifiable pollen grains of very poor quality preservation; (v) Assemblages containing a mixture of types ii-iv above (e.g. argillaceous halite samples containing well-preserved intact palynomorphs as well as highly degraded Unidentifiable grains).

The evaporite palynomorph assemblages are of particular interest because they contain a mixture of pollen preservation types, which can be explained by two preservational processes. Well-preserved, intact palynomorphs were likely blown to the site of deposition on the wind, settled on the surface of the super-saturated sea water where they were encapsulated in the rapidly growing halite crystals. Poorly preserved pollen grains originate from clayey or argillaceous layers/pockets within the salt and arrived at the site of deposition via different means, having been subjected to higher degrees of biological degradation. Some may have washed in from the land via rivers or streams. Others may have settled out from the marine water column. While reworking within individual halite units is a possibility due to the high mobility of halite, the possibility of reworking between evaporite units is discounted based on the relative immobility of anhydrite and potassium-magnesium salts which constrain the more mobile layers of halite. The preservation potential of the Zechstein evaporites is discussed in more detail in Gibson and Bodman (2020).

The dark colour of palynomorphs in some assemblages (particularly Type (ii) above) is a curious matter. Across EZ1-5 an apparent reverse thermal maturity profile indicated by

1193 palynomorph colour is observed with older assemblages being paler and more translucent than
1194 younger ones. Instead of being a true reverse thermal maturity profile darkening may be a result
1195 of the thermal conductivity of evaporites in combination with the exposure of palynomorphs
1196 to a hypersaline environment. It is also be a taphonomic effect of palynomorphs from the Marl
1197 Slate of the Durham Sub-basin which are exceptionally hyaline in appearance, possibly due to
1198 the more basinward location of the Durham Sub-basin.

1199

1200 **8. Conclusions**

1201 Euramerica during the Permian was characterised by a progressive trend towards more
1202 arid climates (Roscher and Schneider, 2006; Montañez et al., 2007). However, the semi-arid
1203 climates of the Zechstein Basin were punctuated by several periods of more humid conditions
1204 associated with marine transgressions.

1205 Spore-pollen preservation potential is highest during transgressive phases and just
1206 before regressive phases (e.g. Kustatscher et al., 2017). Other points of cycles fall outside of
1207 this taphonomic window of preservation, resulting in a reduced recovery of palynomorph. The
1208 use of evaporite palynology helps compensate for this, providing insight into the regressive
1209 phase flora for the first time.

1210 Pollen-dominated assemblages have been recovered from throughout the Zechstein
1211 Group. Assemblages are dominated by conifer pollen, reflecting the characteristics of the
1212 gymnospermous Euramerican parent flora. The composition of assemblages remains relatively
1213 unchanged, both within and between Zechstein cycles. This confirms the reported uniform
1214 nature of the Zechstein vegetation.

1215 Despite the additional taphonomic window afforded by the evaporites there remains
1216 difficulties disentangling taphonomic effects from biological signals. Regardless, the
1217 gymnospermous inland and hinterland flora appears to have persisted throughout the course of
1218 Zechstein deposition at least until the sea finally disappeared at or close to the Permian-Triassic
1219 boundary.

1220

1236

**SUPPORTING INFORMATION**

Additional Supporting Information can be found in the online version of this article:

Appendix A. Lithostratigraphical and facies descriptions for all localities

Appendix B. List of borehole samples, their lithology, and yield

Appendix C. List of outcrop samples, their lithology, and yield

Appendix D. Location and stratigraphic range of all localities

Appendix E. Raw count data

**References**

Afonin, S.A., Barinova, S.S., Krassilov, V.A., 2001. A bloom of *Tympanicysta* Balme 1980 (green algae of zygnematalean affinities) at the Permian–Triassic boundary. Geodiversitas 23, 481–487.

Anderson, J.M., Anderson, H.M., 1983. Palaeoflora of southern Africa, Molteno Formation (Triassic) 1. (Part 1. Introduction; Part 2. Dicroidium). Balkema, Rotterdam.

Archangelsky, S., Wagner, R.H., 1983. *Glosspteris anatolica* sp. nov. from uppermost Permian strata in south east Turkey. Bulletin of the British Museum (Natural History). Geology 37, 81–91.

Balme, B.E., 1995. Fossil in situ spores and pollen grains: an annotated catalogue. Review of Palaeobotany and Palynology 87, 81–323.

Bauer, K., Kustatscher, E., Butzmann, R., Fischer, T.C., van Konijnburg-van Cittert, J.H.A., Krings, M., 2014. Ginkgophytes from the Upper Permian of the Bletterbach Gorge (Northern Italy). *Rivisita Italiana di Paleontologia e Stratigrafia* 120(3), 271-279.

Benton, M.J., Twitchett, R.J., 2003. How to Kill (Almost) All Life: The End-Permian Extinction Event. Trends in Ecology and Evolution 18(7), 358–365.

Bercovici, A., Diez, J.B., Broutin, J., Bourquin, S., Linol, B., Villanueva-Amadoz, U., López-Gómez, J., Durand, M., 2009. A palaeoenvironmental analysis of Permian sediments in Minorca (Balearic Islands, Spain) with new palynological and megafloral data. Review of Palaeobotany and Palynology 158, 14–28.

Berridge, N.G., Pattison, J., Samuel, M.D.A., Brandon, A., Howard, A.S., Pharaoh, T. C., Riley, N.J., 1999. Geology of the Grantham district. Memoir of the British Geological Survey 127, 1-133.

Bomfleur, B., Serbet, R., Taylor, E.L., Taylor, T.N. 2011. The possible pollen cone of the Late Triassic conifer *Heidiphyllum/Telemachus* (Voltziales) from Antarctica. Antarctic Science 23, 379–385.

Brauns, C.M., Pätzold, T., Haack, U., 2003. A Re-Os study bearing on the age of the Kupferschiefer at Sangerhausen (Germany). International Congress on Carboniferous and Permian Stratigraphy, Utrecht, August 2003, 66 pp.

Chaloner, W.G., 2013. Three Palynological Puzzles. International Journal of Plant Sciences 174(3), 602-607.

1276 Clarke, R.F.A., 1965. British Permian saccate and monosulcate miospores. Palaeontology 8,
1277 322–354.

1278 Clayton, G. Goodhue, R., Adelbagi, S. T., Vecoli, M., 2017. Correlation of Palynomorph
1279 Darkness Index and vitrinite reflectance in a submature Carboniferous well section in northern
1280 Saudi Arabia. Revue de Micropaléontologie 60, 411–416 ARAMCO-CIMP.

1281 Cleal, C.J., Thomas, B.A., 1995. Palaeozoic Palaeobotany of Great Britain, Geological
1282 Conservation Review Series, No. 9, Chapman and Hall, London, 295 pp.

1283 Clement-Westerhof, J.A., 1984. Aspects of Permian palaeobotany and palynology. IV. The
1284 conifer Ortiseia Florin from the Val Gardena Formation of the Dolomites and the Vicentinian
1285 Alps (Italy) with special reference to a revised concept of the Walchiaceae (Göppert) Schimper.
1286 Review of Palaeobotany and Palynology 41, 51-166.

1287 Clement-Westerhof, J.A., 1987. Aspects of Permian palaeobotany and palynology. VII. The
1288 Majonicaceae, a new family of Late Permian conifers. Review of Palaeobotany and Palynology
1289 52, 375–402.

1290 Clement-Westerhof, J.A., 1988. Morphology and phylogeny of Paleozoic conifers. 298-337.
1291 In: Beck, C. (Ed.), Origin and Evolution of Gymnosperms. Columbia University Press, New
1292 York, 504 pp.

1293 Doornenbal, J.C., Stevenson, A.G. (Eds.) 2010. Petroleum Geological Atlas of the Southern
1294 Permian Basin Area. EAGE Publications b.v., Houten, 342 pp.

1295 Elsik, W.C., 1999. *Reduviasporonites* Wilson 1962: Synonymy of the Fungal Organism
1296 Involved in the Late Permian Crisis. American Association of Stratigraphic Palynologists 23,
1297 27-41.

1298 Erwin, D.H., 1993. The Great Paleozoic Crisis: Life and Death in the Permian. Columbia
1299 University Press, New York. 327 pp.

1300 Erwin, D.H., 2006. Extinction: How Life on Earth Nearly Ended 250 Million Years Ago.
1301 Princeton University Press, Princeton, New Jersey. 296 pp.

1302 Florin, R., 1944. Die Koniferen des Oberkarbons und des Unteren Perms. Palaeontographica
1303 Abteilung B-Palaophytologie 85, 365–456.

1304 Foster, C.B., Afonin, S.A. 2005. Abnormal pollen grains: an outcome of deteriorating
1305 atmospheric conditions around the Permian-Triassic boundary. Journal of the Geological
1306 Society of London 162, 653-659.

1307 Foster, C.B., Stephenson, M.H., Marshall, C., Logan, G.A., Greenwood, P. F. 2002. A Revision
1308 of *Reduviasporonites* Wilson 1962: Description, Illustration, Comparison and Biological
1309 Affinities. American Association of Stratigraphic Palynologists 26, 35-58.

1310 García-veigas, J., Cendón, D.I., Pueyo, J.J., Peryt, T. M., 2011. Zechstein saline brines in
1311 Poland, evidence of overturned anoxic ocean during the Late Permian mass extinction event.
1312 Chemical Geology 290, 189-201.

1313 Geinitz, H.B., 1869. Über fossile Pflanzenreste aus der Dyas von Val Trompia. Neues Jahrbuch
1314 für Mineralogie, Geologie and Paliontologie 456-461.

1315 Geluk, M., 1999. Late Permian (Zechstein) rifting in the Netherlands: models and implications
1316 for petroleum geology. Petroleum Geoscience 5, 189–199.

Gibson, M.E., Taylor, W.A., Wellman, C.H., 2020. Wall ultrastructure of the Permian pollen grain *Lueckisporites virkkiae* Potonié et Klaus 1954 emend. Clarke: Evidence for botanical affinity. Review of Palaeobotany and Palynology 275, 104169.

Gibson, M.E. Bodman, D., 2020. Evaporite palynology of the British Zechstein salts: a method for processing all evaporite types. In review.

Geluk, M. 2005. Stratigraphy and tectonics of Permo-Triassic basins in the Netherlands and surrounding areas. Unpublished PhD Thesis, Utrecht University.

Glennie, K.W., 1983. Early Permian (Rotliegendes) Palaeowinds of the North Sea. Sedimentary Geology 34, 245–265.

Glennie, K.W. and Buller, A., 1983. The Permian Weissliegend of N.W. Europe: the partial deformation of aeolian sand caused by the Zechstein transgression. Sedimentary Geology 35, 43-81.

Gomankov, A. V., Meyen, S. V., 1986. Tatarian flora (composition and distribution in the Late Permian of Eurasia). Nauka, Moscow. 175 (in Russian).

Goodhue, R., Clayton, G., 2010. Palynomorph darkness index (PDI) - A new technique for assessing thermal maturity. Palynology 34(2), 147-156.

Gothan, W., Gimm, O., 1930. Neuere Beobachtungen und Betrachtungen über die Flora des Rotliegenden in Thüringen. Arb Inst Palaeobot Petrograph Brennsteile 2, 39–74.

Gotahn, W., Nagalhard, K., 1921. Kupferschieferpflanzen aus dem niederrheinischen Zechstein. Jahrbuch der Königlich Preussischen Geologischen Landesanstalt und Bergakademie 42, 440–460.

Gould, R.E., Delevoryas, T., 1977. The biology of *Glossopteris*: evidence from petrified seed-bearing and pollen-bearing organs. Alcheringia 1, 387–399.

Grauvogel-Stamm, L., 1978. La flore du Grès à Voltzia (Buntsandstein súperieur) des Vosges du Nord (France). Morphologie, anatomie, interprétations phylogénique et paléogéographique. Université Louis-Pasteur de Strasbourg Institut de Géologie 50, 1-225.

Grauvogel-Stamm, L., Doubinger, J., 1975. Deux fougères fertiles du Stéphanien du Massif Central (France). Geobios, 6, 409–421.

Grauvogel-Stamm, L., Grauvogel, L., 1973. *Masculostrobus acuminatus* nom. nov., un nouvel organe reproducteur mâle de Gymnosperme de Grès à Voltzia (Trias inférieur) des Vosges (France). Geobios 6, 101–114.

Hallam, A., Wignall, P. B. 1997. Mass Extinctions and their Aftermath. Oxford University Press, Oxford, 320 pp.

Haubold, H., Schaumberg, G., 1985. Die Fossilien des Kupferschiefer: Pflanzen-und Tierwelt zu Beginn des Zechsteins; eine Erzlagerstatte und ihre Palaontologie. Wittenberg Lutherstadt. 223 pp.

Hauke, R.L., 1963. A taxonomic monograph of the genus *Equisetum* subgenus *Hippochaete*. Nova Hedwigia 8, 1-123.

Hernandez-Castillo, G.R., Rothwell, G.W., Mapes, G., 2001. Thucydiaceae fam. nov., with a review and reevaluation of Paleozoic walchian conifers. International Journal of Plant Sciences 162, 1155–1185.

Hochuli, P.A., 2016. Interpretation of "fungal spikes" in Permian-Triassic boundary sections. Global and Planetary Change 144, 48-50.

Hug, N., 2004. Sedimentgenese und Paläogeographie des höheren Zechsteins bis zur Basis des Buntsandsteins in der Hessischen Senke. Geologische Abhandlungen Hessen 113, 1–238.

Hug, N. Gaupp, R., 2006. Palaeogeographic reconstruction in red beds by means of genetically related correlation: results from the upper part of the German Zechstein (Late Permian). Zeitschrift der Deutschen Gesellschaft für Geowissenschaften 157, 107–120.

Husby, C., 2013. Biology and functional morphology of *Equisetum* with emphasis on the giant horsetails. Botanical Review 79(2), 147-177.

Käding, K.C., 2000. Die Aller-, Ohre-, Friesland- und Fulda-Folge (vormals Bröckelschiefer-Folge). Kali und Steinsalz 13, 760–770.

Klaus, W., 1963. Sporen aus dem südalpinen Perm. Jahrbuch der Geologischen Bundesanstalt, Wien 106, 229–363.

Kustatscher, E., Konijnenburg-van Cittert, J.H.A. van, Bauer, K., Butzmann, R., Meller, B., Fischer, T.C., 2012. A new flora from the upper Permian of Bletterbach (Dolomites, N-Italy). Review of Palaeobotany and Palynology 182, 1–13.

Kustatscher, E., Bauer, K., Butzmann, R., Fischer, T.C., Meller, B., van Konijnenburg-van Cittert, J.H.A., Kerp, H., 2014. Sphenophytes, pteridosperms and possible cycads from the Wuchiapingian (Lopingian, Permian) of Bletterbach (Dolomites, Northern Italy). Review of Palaeobotany and Palynology 208, 65-82.

Kustatscher, E., Bernardi, M., Petti, F.M., Franz, M., van Konijnenburg-van Cittert, J.H.A., Kerp, H., 2017. Sea-level changes in the Lopingian (late Permian) of the northwestern Tethys and their effects on the terrestrial palaeoenvironments, biota and fossil preservation. Global and Planetary Change 148, 166–180.

Labandiera, C.C., Kustatscher, E., Wappler, T., 2016. Floral assemblages and patterns of insect herbivory during the Permian to Triassic of Northeastern Italy. PLoS ONE 11(11), e0165205.

Legler, B., Gebhardt, U., Schneider, J.W., 2005. Late Permian non-marine-marine transitional profiles in the central Southern Permian Basin, northern Germany. International Journal of Earth Sciences 94(5–6), 851–862.

Legler, B., Schneider, J., 2008. Marine ingressions into the Middle/Late Permian saline lake of the Southern Permian Basin (Rotliegend, Northern Germany) possibly linked to sea-level highstands in the Arctic rift system. Palaeogeography, Palaeoclimatology, Palaeoecology 267(1-2), 102-114.

Lindström, S., McLoughlin, S., Drinnan, A.N., 1997. Intraspecific variation of taeniate bisaccate pollen within Permian glossopterid sporangia, from the Prince Charles Mountains, Antarctica. International Journal of Plant Sciences 158, 673–684.

Marmottant, P., Ponomarenko, A., Bienaimé, D., 2013. The walk and jump of *Equisetum* spores. Proceedings of the Biological Society 280(1770), 20131465.

Menning, M., Gast, R., Hagdorn, H., Käding, K.-C., Simon, T., Szurlies, M., Nitsch, E., 2005. Zeitskala für Perm und Trias in der Stratigraphischen Tabelle von Deutschland 2002, zyklostratigraphische Kalibrierung der höheren Dyas und Germanischen Trias und das Alter der Stufen Roadium bis Rhaetium 2005. Newsletters on Stratigraphy 41(1/3), 173–210.

Menning, M., Alekseev, A.S., Chuvashov, B.I., Davydov, V.I., Devuyst, F.X., Forke, H.C., Grunt, T.A., Hance, L., Heckel, P.H., Izokh, N.G., Jin, Y.G., Jones, P.J., Kotlyar, G.V., Kozur, H.W., Nemyrovska, T.I., Schneider, J.W., Wang, X.D., Weddige, K., Weyer, D., Work, D.M., 2006. Global time scale and regional stratigraphic reference scales of Central and West Europe, East Europe, Tethys, South China, and North America as used in the Devonian–Carboniferous–Permian Correlation Chart 2003 (DCP 2003). Palaeogeography, Palaeoclimatology, Palaeoecology 240, 318–372.

Metcalfe, I., Foster, C.B., Afonin, S.A., Nicoll, R.S., Mundil, R., Xiaofeng, W., Lucas, S.G. 2009. Stratigraphy, biostratigraphy and C-isotopes of the Permian–Triassic non-marine sequence at Dalongkou and Luaogou, Xinjiang Province, China. Journal of Asian Earth Sciences 36, 503–520.

Meyen, S.V., 1997. Permian conifers of western Anagaraland. Review of Palaeobotany and Palynology 96, 351–447.

Meyen, S.V., 1984. Basic features of gymnosperm systematics and phylogeny as shown in the fossil record. The Botanical Review 50, 1–111.

Naugolnykh, S.V., 2014. A new genus of male cones of voltzialean affinity, *Uralostrobus voltzioides* nov. gen., nov. sp., from the Lower Permian of the Urals (Russia). Geobios 47, 315-324.

Massari, F., Conti, M.A., Fontana, D., Helmold, K., Mariotti, N., Neri, C., Nicosia, U., Ori, G.G., Pasini, M., Pittau, P., 1988. The Val Gardena Sandstone and BellerophonFormation in the Bletterbach gorge (Alto Adige, Italy): biostratigraphy and sedimentology. Memorie di Scienze Geologiche 40, 229–273.

Massari, F., Neri, C., Pittau, P., Fontana, D., Stefani, C., 1994. Sedimentology, palynostratigraphy and sequence stratigraphy of a continental to shallow-marine rift-related succession: Upper Permian of the eastern Southern Alps (Italy). Mem. Sci. Geol. 46, 119–243.

Massari, F., Neri, C., Fontana, D., Manni, R., Mariotti, N., Nicosia, U., Pittau, P., Spezzamonte, M., Stefani, C., 1999. Excursion 3: The Bletterbach section (Val Gardena Sandstone and Bellerophon Formation), in: Stratigraphy and Facies of the Permian Deposits between Eastern Lombardy and Western Dolomites - Field Trip Guidebook. Presented at the International Fiel Conference on "The Continental Permian of the Southern Alps and Sardinia (Italy). Regional Reports and General Correlations," Brescia, Italy, pp. 111–134.

Osborn, J.M., Taylor, T.N., 1993. Pollen morphology and ultrastructure of the Corystospermales: permineralized in situ grains from the Triassic of Antarctica. Review of Palaeobotany and Palynology 79, 205–219.

Pancost, R.D., Crawford, N., Maxwell, J.R., 2002. Molecular evidence for basin-scale photic zone euxinia in the Permian Zechstein Sea. Chemical Geology 188, 217–227.

Pattison, J., Smith, D.B., Warrington, G., 1973. A review of Late Permian and Early Triassic biostratigraphy in the British Isles. 220-260. In: Logan, A., Howse, L.V. (eds), 1973. The Permian and Triassic Systems and their Mutual Boundary. Memoir (Canadian Society of Petroleum Geologists) 2, 766 pp.

Paul, J., 2006. Der Kupferschiefer: Lithologie, Stratigraphie, Fazies und Metallogenese eines Schwarzschiefers. Zeitschrift der Deutschen Gesellschaft für Geowissenschaften 157, 57–76.

Peryt, T.M., Geluk, M.C., Mathiesen, A., Paul, J., Smith, K., 2010. Zechstein. 123-147. In: Doornenbal, J. C., Stevenson, A. G. (Eds.) Petroleum Geological Atlas of the Southern Permian Basin Area. EAGE Publications b.v., Houten, 342 pp.

Peryt, T. Raczyński, P., Peryt, D. and Chłódek, K., 2012. Upper Permian reef complex in the basinal facies of the Zechstein Limestone (Ca1), western Poland. Geological Quarterly 47, 537-533.

Pittau, P., 1999. Excursion 3: the Bletterbach section (Val Gardena Sandstone and Bellerophon Formation). 3. Palynology. Stratigraphy and facies of the Permian deposits between Eastern Lombardy and the Western Dolomites. Field trip guidebook 23–25.

Pittau, P., Kerp, H., Kustatscher, E., 2005. "Let us meet across the P/T boundary"—workshop on Permian and Triassic Palaeobotany and Palynology, Bozen. The Bletterbach canyon. Naturmuseum Südtirol/Museo Scienze Naturali Alto Adige/Museum Natöra Südtirol, p. 26.

Podoba, B.G. 1975. Spores and pollen. In: Suveizdis, P. (ed.), Permian deposits of the Baltic area (stratigraphy and gauna); Lietuvos Geologijos Mokslinio Tyrimo Institutas, Darbai, Mintis, Vilnius 29, 184-192 (In Russian; English summary p. 196-207).

Poort, R.J., Kerp, H., 1990. Aspects of Permian palaeobotany and palynology XI. On the recognition of true peltasperms in the Upper Permian of western and central Europe and a reclassification of species formerly included in Peltaspermum Harris. Review of Palaeobotany and Palynology 63, 197-225.

Poort, R. J., Clement-Westerhof, J.A., Looy, C.V., and Visscher, H., 1997. Aspects of Permian palaeobotany and palynology XVII. Conifer extinction in Europe at the Permian-Triassic junction: Morphology, ultrastructure and geographic/stratigraphic distribution of Nuskoisporites dulhuntyi (prepollen of Ortiseia, Walchiaceae). Review of Palaeobotany and Palynology 97(1-2), 9-39.

Potonié, R., 1962. Synopsis der Sporae in situ. Beihefte zum Geologische Jahrbuch 52, 1–204.

Raine, J.I., Mildenhall, D.C., Kennedy, E.M., 2011. New Zealand Fossil Spores and Pollen: An Illustrated Catalogue, 4th edition. GNS Science miscellaneous series no. 4.

Retallack, G.J., 2002. *Lepidopteris callipteroides*, an early Triassic seedfern of the Sydney Basin, southeastern Australia. Alcheringa 1, 475–500.

Richter-Bernburg, G., 1955. Stratigraphische Gliederung des deutschen Zechstein. Zeitschrift für Geologische Wissenschaften 105, 843–854.

Röhling, H.-G., 1993. Der Untere Buntsandstein in Nordwest- und Nordostdeutschland – Ein Beitrag zur Vereinheitlichung der stratigraphischen Nomenklatur. Geologisches Jahrbuch A 142, 149–183.

Rothwell, G. W., Mapes, G. and Hernandez-Castillo, G. R., 2005. *Hanskerpia* gen. nov. and phylogenetic relationships among the most ancient conifers (Voltziales). Taxon 54, 733–750.

Schweitzer, H.-J., 1960. Die Makroflora des niederrheinischen Zechsteins. Fortschritte Geologisches Rheinland Westfalen 6, 1–46

Schweitzer, H.-J., 1968. Die Flora des Oberen Perms in Mitteleuropa. Naturwissenschaften Rundschau 21, 93–102.

Schweitzer, H.-J., 1986. The land flora of the English and German Zechstein sequences. In: Harwood, G.M., Smith, D.B. (eds) The English Zechstein and Related Topics. Geological Society, London, Special Publications 22, 31–54.

Słowakiewicz, M., Kiersnowski, H., Wagner, R. 2009. Correlation of the Middle and Upper Permian marine and terrestrial sedimentary sequences in Polish, German, and USA Western Interior Basins with reference to global timemarkers. Palaeoworld 18, 193–211.

Smith, D.B., Brunstrom, R.G.W., Manning, P.I., Simpson, S., Shotton, F.W., 1974. A Correlation of the Permian Rocks of the British Isles. Geological Society, London, Special Reports 5, 45 pp.

Smith, D.B., 1989. The late Permian palaeogeography of north-east England. Proceedings of the Yorkshire Geological Society 47, 285-312.

Solms-Laubach, H. Graf Von, 1884. Die Coniferenformen des deutschen Kupferschiefers und Zechsteins. Palaeontologische Abhandlungen 2(2), 81–116.

Spina, A., Cirilli, S., Utting, J. and Jansonius, J., 2015. Palynology of the Permian and Triassic of the Tesero and Bulla sections (Western Dolomites, Italy) and consideration about the enigmatic species *Reduviasporonites chalastus*. Review of Palaeobotany and Palynology 218, 3–14.

Stephenson, M.H., 2018. Permian palynostratigraphy: a global overview. Geological Society Special Publication 450(1), 321-347.

Stone, P., Milward, D., Young, B., Merritt, J.W., Clarke, S.M., McCormac, M., Lawrence, D.J.D., 2010. British regional geology: Northern England. Fifth edition. Keworth, Nottingham: British Geological Survey. 307 pp.

Stoneley, H.M.M., 1958. The Upper Permian flora of England. Bulletin of the British Museum (Natural History) Geology 3(9), 293-337.

Szurlies, M., 2013. Late Permian (Zechstein) magnetostratigraphy in Western and Central Europe. Geological Society, London, Special Publication 376, 73-85.

Taylor T.N., Taylor, E.L., Krings, M., 2009. Paleobotany. 2nd ed. Elsevier, Amsterdam.

Tucker, M., 1991. Sequence stratigraphy of carbonate-evaporite basins; models and application to the Upper Permian (Zechstein) of Northeast England and adjoining North Sea. Journal of the Geological Society of London 148, 1019-1036.

Ulh, D., Kerp, H., 2002. Preservation of fossil plants from the Zechstein (Upper Permian) of Central Europe. Freiberger Forschungshefte 497(January), 29-43.

Variakhuna, L.M., 1971. Spores and pollen of the red beds and coal deposits of the Permian and Triassic of the northeastern region of the USSR; Akademiia Nauk SSSR, Komi Filial, Institut Geologii, Nauka, Leningrad, 158p., pl. I-IVIII + 1-44 p. (in Russian).

Van Wees, J.-D., Stephenson, R.A., Ziegler, P.A., Bayer, U., Mccann, T., Dadlex, R., Gaupp, R., Narkiewicz, M., Bitzer, F., Scheck, M., 2000. On the origin of the Southern Permian Basin, Central Europe. Marine and Petroleum Geology 17, 43-59.

Visscher, H., 1971. The Permian and Triassic of the Kingscourt Outlier, Ireland. Special Papers of the Geological Society of Ireland 1, 1-104.

1524 Visscher, H., Brinkhuis, H., Dilcher, D.L., Elsik, W.C., Eshet, Y., Looy, C.V., Rampino, M.
1525 R., Traverse, A., 1996. The terminal Paleozoic fungal event: Evidence of terrestrial ecosystem
1526 destabilization and collapse. National Academy of Sciences Proceedings 93, 2155–2158.

1527 Visscher, H., Sephton, M.A., Looy, C.V., 2011. Fungal virulence at the time of the end-
1528 Permian biosphere crisis? Geology 39(9), 883-886.

1529 Wagner, R., Peryt, T.M., 1997. Possibility of sequence stratigraphic subdivision of the
1530 Zechstein in the Polish Basin. Geological Quarterly 41, 457–474.

1531 Wall, D., Downie, C., 1963. Permian hystrichospheres from Britain. Palaeontology 5, 770-784.

1532 Warrington, G., Scrivener, R.C. ,1988. Late Permian fossils from Devon: regional geological
1533 implications. Proceedings of the Usher Society 7, 95-96.

1534 Warrington, G. 2005. The chronology of the Permian and Triassic of Devon and south-east
1535 Cornwall (UK): a review of methods and results. Geoscience in south-west England 11, 117-
1536 122.

1537 Warrington, G., 2008. Palynology of the Permian succession in the Hilton Borehole, Vale of
1538 Eden, Cumbria, UK. Proceedings of the Yorkshire Geological Society 57(2), 123-130.

1539 Weigelt, J., 1928. Die Pflanzenreste des mitteldeutschen Kupferschiefers und ihre Einschaltung
1540 ins Sediment – Eine palökologische Studie. Fortschritte der Geologie und Paläontologie, VI
1541 19, 395–592.

1542 Whitaker, D.L., Edwards, J., 2010. Sphagnum moss disperses spores with vortex rings. Science
1543 329, 406.

1544 Zavada, M.S., Crepet, W.L., 1985. Pollen wall ultrastructure of the type material of *Pteruchus*
1545 *africanus*, *P. dubius* and *P. papillatus*. Pollen Spores 27, 271–276.

1546 Zavialova, V., Nosova, N., Gavrilova, O., 2016. Pollen grains associated with gymnospermous
1547 mesofossils from the Jurassic of Uzbekistan. Review of Palaeobotany and Palynology 233,
1548 125-145.

1549 Zavada, M.S., 1991. The ultrastructure of pollen found in dispersed sporangia of *Arberiella*
1550 (Glossopteridaceae). Botanical Gazette 152, 248–255.

1551 Ziegler, A.M., 1990. Phytogeographic patterns and continental configurations during the
1552 Permian period. Palaeozoic Palaeogeography and Biogeography, McKerrow, W.S., Scotese,
1553 C.R. (Eds.), Memoirs of the Geological Society 12, 363-379.

1554

1555

1556

1557

1558

1559

1560

1561

**Plate I**

1

2

3

4

5

6

7

8

9

10

11

12

13

14

15

17

16

18
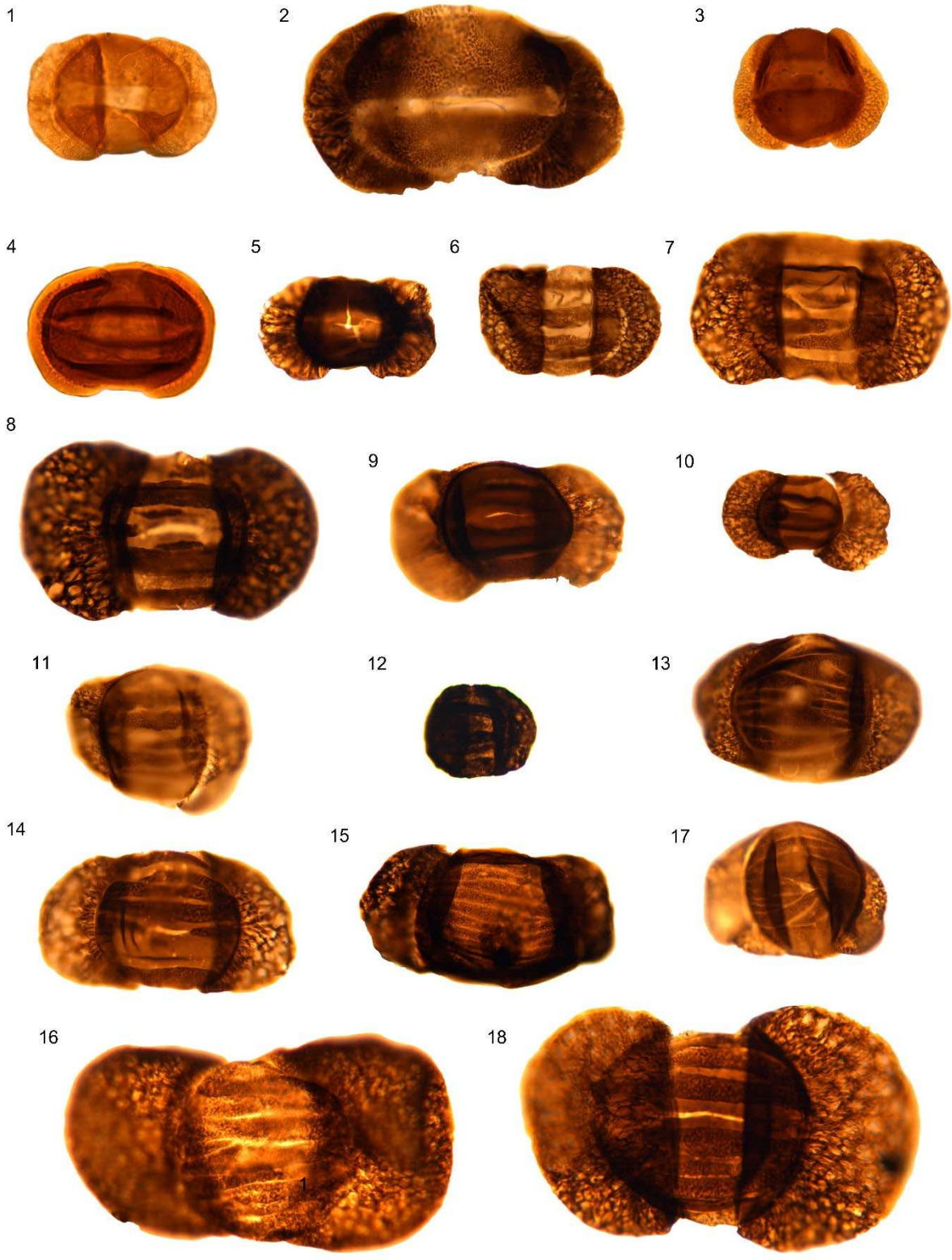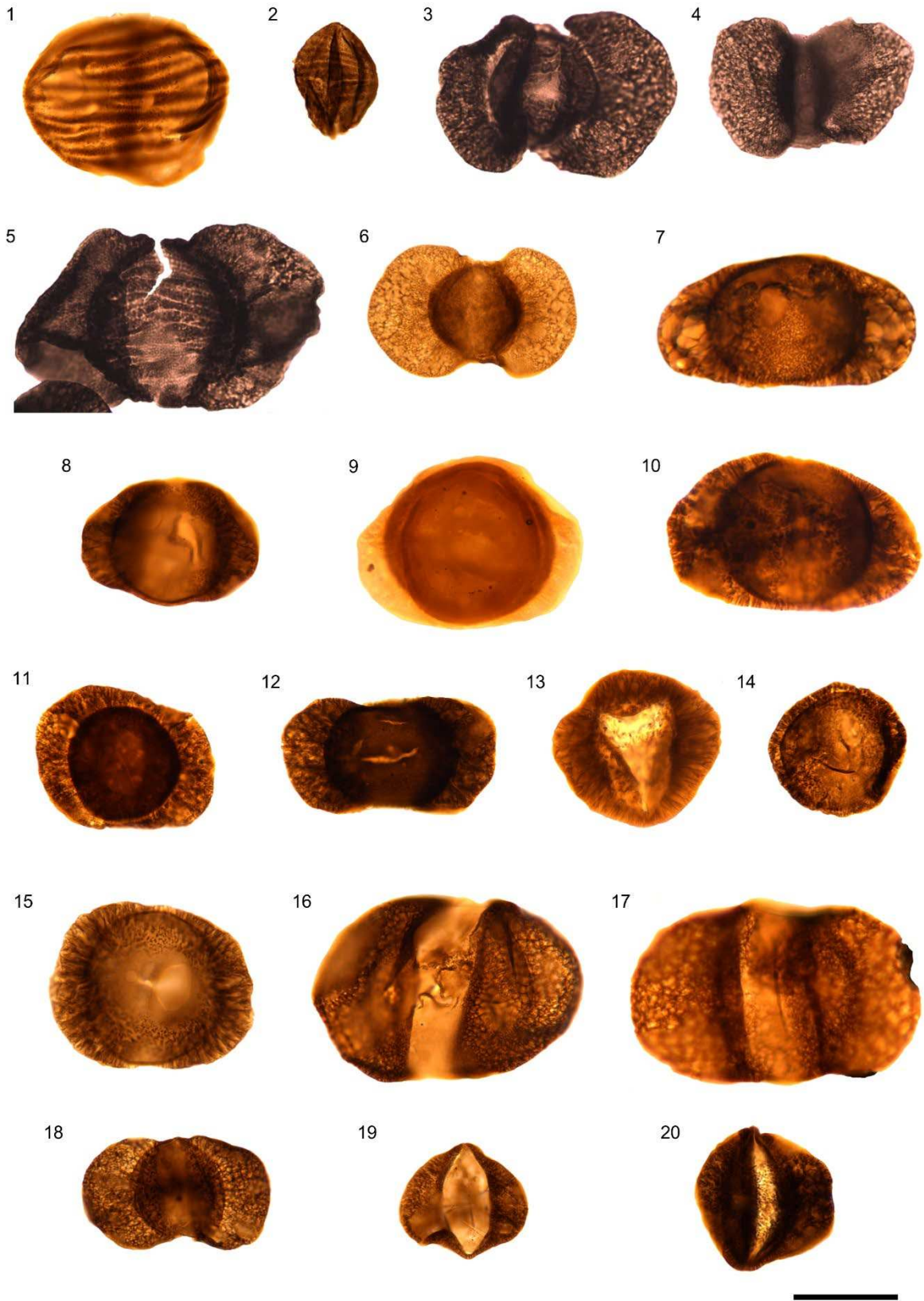
*Plate II*

# Plate III

**Plate Descriptions**

Plate I. Taeniate bisaccate pollen grains. England Finder co-ordinates included. Scale bar represents 50 μm in all images. Images taken using a QImaging (Model No. 01-MP3.3-RTV-R-CLR-10) camera mounted on an Olympus BH-2 transmitted light microscope in conjunction with QCapture Pro software.

1. *Lueckisporites virkkiae* Variant A (KIM 5, P43)
2. *L. virkkiae* Variant A (SM11 1312.24 m, U42/1)
3. *L. virkkiae* Variant B (KIM 5, B33/1)
4. *L. virkkiae* Variant C (KIM 6, E36/1)
5. *L. virkkiae* Variant C (SM11 1312.24 m, K30/1)
6. *Taeniaesporites labdacus* (SM11 1312.24 m, W45/2)
7. *T. labdacus* (SM11 1312.24 m, J32/2)
8. *T. noviaulensis* (SM11 1312.24 m, R42)
9. *T. noviaulensis* (SM11 1312.24 m, M48/2)
10. *T. novimundi* (SM11 1312.24 m, S31/2)
11. *T. angulistriatus* (SM1 1312.24 m, V35/3)
12. *T. albertae* (SM11 1458.37 m, J46/3)
13. *Protohaploxypinus chaloneri* (SM11 1312.24 m, G30)
14. *P. chaloneri* (SM11 1312.24 m, R36/3)
15. *P. jacobii* (SM11 1312.24 m, S46)
16. *P. jacobii* (SM11 1312.24 m, L33/1))
17. *P. microcorpus* (SM11 1312.24 m, K33)
18. *P.* cf. *samoilovichii.* (SM11 1334.10 m, O39)

Plate II. Taeniate and non-taeniate bisaccate pollen and monosaccate pollen. . England Finder co-ordinates included. Scale bar represents 50 μm for all images. Images taken using a QImaging (Model No. 01-MP3.3-RTV-R-CLR-10) camera mounted on an Olympus BH-2 transmitted light microscope in conjunction with QCapture Pro software.

1. *Vittatina hiltonensis* (SM11 1312.24 m, F31)
2. *V. hiltonensis* (M4 1438.07 m, H32/2)
3. *Striatoabieites richteri* (SM11 1312.24 m, K27/3)
4. *Striatopodocarpites antiquus* (SM11 1312.24 m, P27)
5. *S. fusus* (SM11 1312.24 m, M29)
6. *Platysaccus radialis* (SM11 1312.24 m, J33/4)
7. *Klausipollenites schaubergeri* (SM11 1312.24 m, T39/3)
8. *K. schaubergeri* (SM11 1312.24 m, D32/3)
9. *Vestigisporites minutus* (KIM 5, P41)
10. *V. minutus* (SM11 1312.24 m, L30)
11. *V. minutus* (SM11 1312.24 m, J44/2)
12. *Illinites delasaucei* (SM11 1312.24 m, V41)
13. *I. klausi* (SM11 1328.76 m, P31/4)
14. *I. tectus* (SM11 1312.24 m, K30)
15. *I. tectus* (SM11 1312.24 m, Q41)
16. *Falcisporites zapfei* (SM11 1312.24 m, H42)
17. *F. zapfei* (SM11 1312.24 m, M33/2)
18. *Alisporites nuthallensis* (SM11 1312.24 m, M45)
19. *Labiisporites granulatus* (SM11 1312.24 m, L41)
20. *L. granulatus* (SM11 1312.24 m, G48/3)

21. *Alisporites nuthallensis* (SM11 1312.24 m, M45)

Plate III. Monosaccate pollen grains, trilete spores and foraminiferal test linings. England Finder co-ordinates included. Scale bar represents 50 μm for all images. Images taken using a QImaging (Model No. 01-MP3.3-RTV-R-CLR-10) camera mounted on an Olympus BH-2 transmitted light microscope in conjunction with QCapture Pro software.

1. *Nuskoisporites* cf. *rotatus* (SM11 1328.76 m, E43)
2. *N. dulhuntyi* (SM11 1312.24 m, T35/3)
3. *Perisaccus granulosus* (SM11 1312.24 m, W35/3)
4. *P. granulosus* (SM11 1312.24 m, O43/1)
5. *Potonieisporites novicus* (SM11 1304.14 m, E31)
6. ?*Potonieisporites novicus* (1312.24 m, D32/2)
7. *Crustaesporites globosus* (SM11 1328.76 m, R40/1)
8. Trilete spore (SM11 1465.92 m, P39)
9. Trilete spore (SM11 1465.92 m, C31/4)
10. Foraminiferal test lining (LSSC3, C37/4)
11. Foraminiferal test lining (SFYFP6373, S48)

Table 1. List of the taxa encountered during this study and their probable botanical affinities.

Table 2. Summary of the distribution of the taxa encountered during this study.